Journal of Medicinal Chemistry

Article

pubs.acs.org/jmc

Synthesis and Biological Evaluation of Tylophorine-Derived Dibenzoquinolines as Orally Active Agents: Exploration of the Role of Tylophorine E Ring on Biological Activity

Yue-Zhi Lee,[†] Cheng-Wei Yang,[†,‡] Hsing-Yu Hsu,[†] Ya-Qi Qiu,[†,‡] Teng-Kuang Yeh,[†] Hsin-Yu Chang,[†] Yu-Sheng Chao,[†] and Shiow-Ju Lee*[,†]

[†]Institute of Biotechnology and Pharmaceutical Research, National Health Research Institutes, No. 35 Keyan Road, Zhunan Town, Miaoli County 350, Taiwan

[‡]Graduate Program of Biotechnology in Medicine, Institute of Molecular Medicine, National Tsing Hua University, Hsinchu, Taiwan

Supporting Information

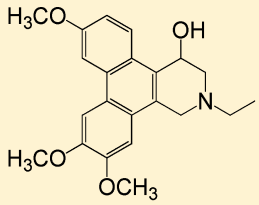

Antiproliferative activity, GI_{50} = 0.02-0.06 μM (NCI-H460, MCF7, HepG2, HONE-1, NUGC-3, and A549)
Anti-TGEV activity, EC_{50} = 0.04 μM
Suppressing NO production in LPS/IFNγ stimulated RAW264.7 cells, EC_{50} = 0.07 μM
In *in vivo* efficacy against rat paw edema, inhibition > 60% ($p < 0.002$)
In *in vivo* efficacy against lung A549 xenograft, tumor volume reduction = 61% ($p < 0.001$)

ABSTRACT: A series of novel tylophorine-derived dibenzoquinolines has been synthesized and their biological activity evaluated. Three assays were conducted: inhibition of cancer cell proliferation, inhibition of TGEV replication for anticoronavirus activity, and suppression of nitric oxide production in RAW264.7 cells (a measure of anti-inflammation). The most potent compound from these assays, dibenzoquinoline **33b**, showed improved solubility compared to tylophorine **9a**, in vivo efficacies in a lung A549 xenografted tumor mouse model and a murine paw edema model, good bioavailability, and no significant neurotoxicity (as tested by a rota-rod test for motor coordination). This is the first study to explore in detail the role of the tylophorine E ring on biological activity and very strongly suggests that tylophorine-derived dibenzoquinolines merit further development into orally active agents.

INTRODUCTION

Tylophorine is a phenanthroindolizidine alkaloid found in various herbs, some of which, e.g., *Tylophora indica*, *Tylophora atrofolliculata*, and *Tylophora ovata*, are used in the traditional medicines of several countries.[1−3] Although their direct molecular targets are not known,[2,4] they have been found to impart a multitude of biological activities, including anticancer,[5−7] anti-inflammation,[5,6] and anticoronavirus.[8] Cancer cell toxicity is accomplished by interfering in the cell cycle and inhibiting the signaling of the transcriptional factors NF-κB and AP1.[5,7] Their anti-inflammatory activity was found to arise through enhanced phosphorylation of Akt and down-regulation of AP1, thereby suppressing nitric oxide production in LPS/IFNγ stimulated RAW264.7 cells.[5] In TGEV (transmissible gastroenteritis coronavirus) infected ST cells, they inhibit coronavirus induced apoptosis and viral replication.[8]

In addition to the conventional pentacyclic phenanthroindolizidines and phenanthroquinolizidines, the biological activity of nonpentacyclic tylophorine derivatives has also been explored. One class of tylophorine derivatives, the tyloindicine I analogue 7-(4-methoxyphenyl)-6-phenyl-2,3,8,8a-tetrahydroindolizin-5(1*H*)-one (**4**) was proposed to operate through an unknown, novel mechanism of action.[9] Another class of tylophorine derivatives, the phenanthrene-based 9-*N* replaced compounds, e.g., **5**, was proposed to exert anticancer activity through a different mode of action by inactivation of Akt and inhibition of the NF-κB pathway signaling.[10] The direct biological targets of these molecules, however, remain to be elucidated. Furthermore, although they all exert anticancer activity, their pharmacophores (for the molecular recognition by biological macromolecules) are likely differentiated, leading to changes in targeted molecules or mechanism of action.

Development of tylophorine-related novel compounds, e.g., *seco*-tylophorine compounds[9,11] and phenanthrene-based 9-*N* replaced compounds[12,13] (Figure 1), into cytotoxic agents for

Received: May 21, 2012
Published: November 20, 2012

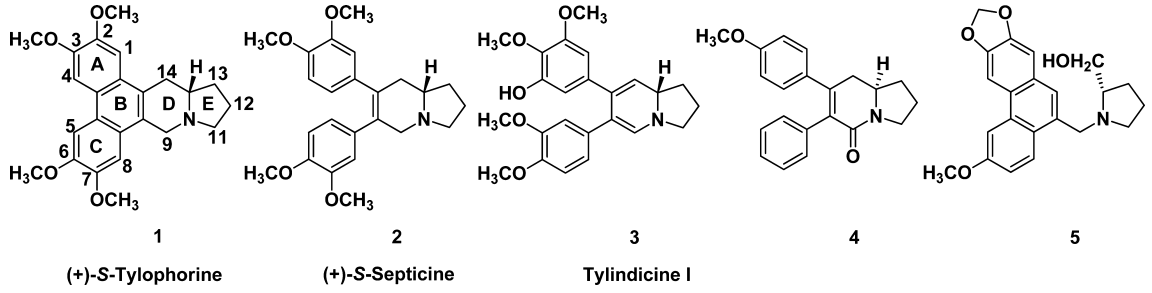

Figure 1. Tylophorine and derived compounds.

Scheme 1. Synthesis of Tylophorine-Derived Dibenzoquinolines with Varied *N*-Substitutes[a]

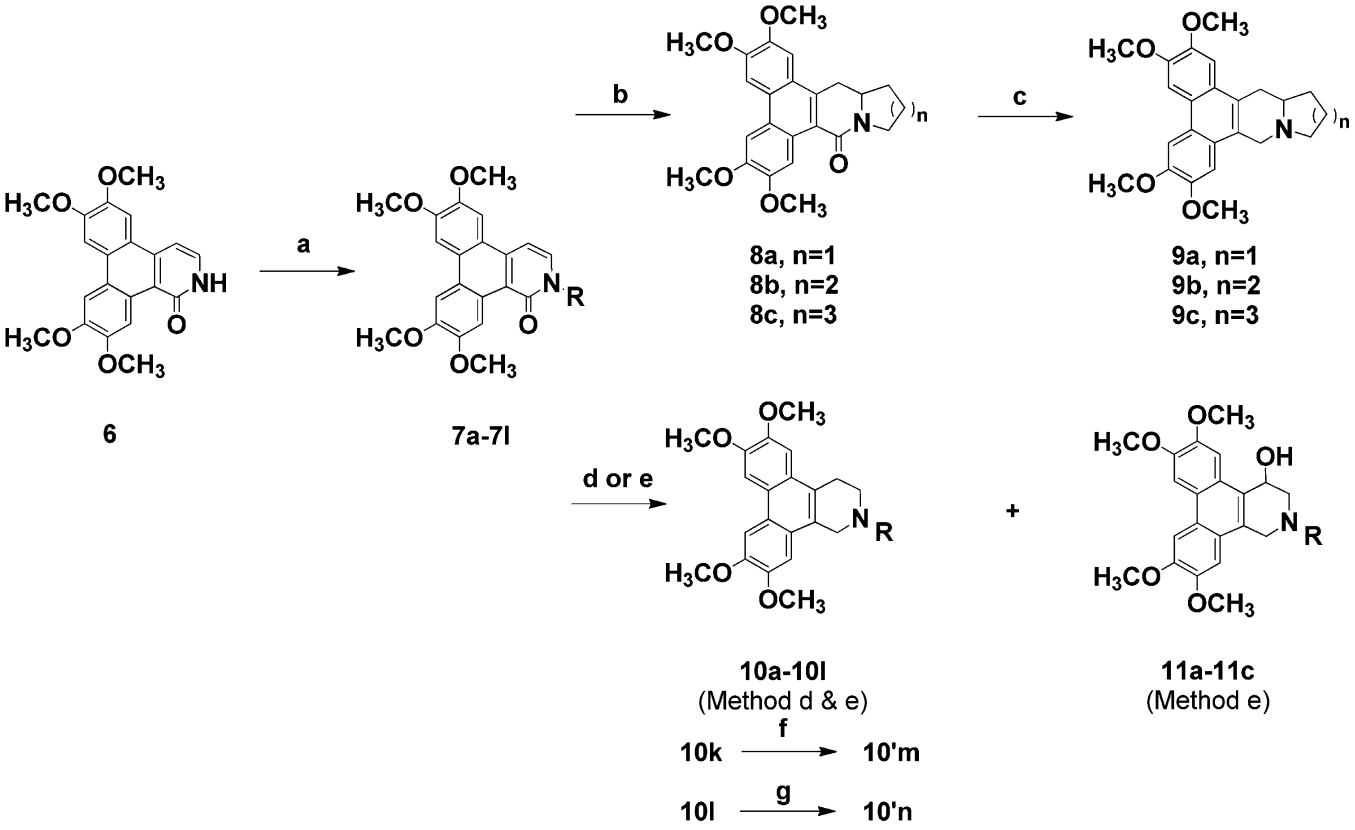

[a]Reagents and conditions: (a) R-Br, NaH, DMF; (b) (i) NaI, CH_3CN, 130 °C, overnight, (ii) Bu_3SnH, AIBN, toluene, reflux, 6 h; (c) $NaAl(OCH_2CH_2OMe)_2H_2$, dioxane, 120 °C, 2 h; (d) $LiAlH_4$, $AlCl_3$, THF, rt, 4 h; (e) $LiAlH_4$, THF, rt, 48 h, quench, MeOH/H_2O (100:1), rt; (f) PPTS, MeOH, 55 °C, 20 h; (g) H_2SO_4, CH_2Cl_2, rt, 20 h.

cancer treatment faces formidable challenges. For example, the solubility of tylophorine in water is very poor. Also, the stereochemistry of these compounds affects their potency[9,14] and thus isolation of enantiopure samples is needed to clarify structure–activity relationships and further development. Furthermore, a clinical trial of tylocrebrine in the 1960s failed due to the central nervous system (CNS) side effects.[15] Increasing the polarity of tylophorine and derived compounds should prevent them from crossing the blood–brain barrier, thereby lowering CNS toxicity. Thus, the solubility, polarity, pharmacokinetic properties, oral availability, neurotoxicity, and synthetic routes toward these compounds must all be improved.

Herein, we investigate the role of the tylophorine E ring (Figure 1) on biological activity through the synthesis of a series of derivatives bearing modifications at the E ring and/or differing *N*-substitutions. All derivatives were submitted for a variety of tests: anticell growth against a panel of cancer cell lines, antiviral replication in TGEV infected ST cells detected by inhibition of TGEV N and S protein expression, and suppression of nitric oxide production in LPS/IFNγ stimulated RAW264.7 cells. The counterpart C13a atom of the E ring-uncyclized derivatives, dibenzoquinolines, is not a stereocenter. Several potent derivatives possessing the same biological activities as tylophorine in terms of anticancer cell proliferation, anti-TGEV activity, and anti-inflammation were discovered and their structure and activity relationships analyzed. Of them, dibenzoquinoline **33b** exhibited improved solubility compared to tylophorine **9a**, potent in vivo efficacy, and good bioavailability as an orally active agent without neurotoxicity.

dx.doi.org/10.1021/jm300705j | J. Med. Chem. 2012, 55, 10363–10377

Scheme 2. Synthesis of Tylophorine-Derived Dibenzoquinolines with Varied Phenanthrene Substitutes[a]

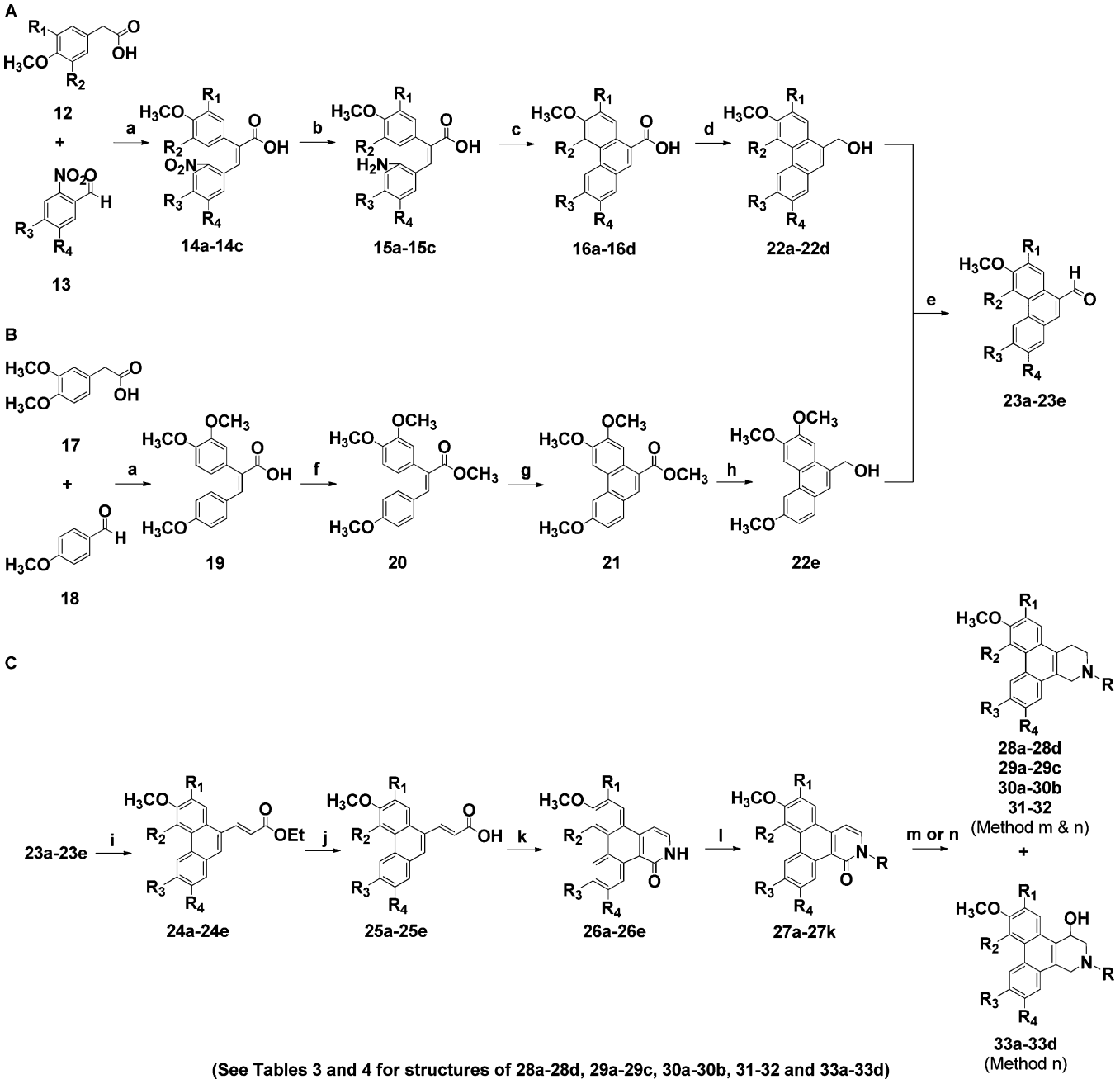

[a]Reagents and conditions: (a) Et_3N, Ac_2O, 90 °C, 15 h; (b) $FeSO_4·7H_2O$, NH_4OH, 100 °C, 2 h; (c) *i*-$C_5H_{11}ONO$, H_2SO_4, NaI, acetone, 0 °C, 6 h; (d) BH_3·THF, THF, 38 °C, 1 h; (e) PCC, CH_2Cl_2, rt, 2 h; (f) H_2SO_4, MeOH, 75 °C, 4 h; (g) $FeCl_3$, CH_2Cl_2, rt, 5 h; (h) $LiAlH_4$, THF, rt, 3 h; (i) $Ph_3P{=}CHCO_2Et$, toluene, reflux, 5 h; (j) KOH, EtOH/H_2O (2:1), reflux, 5 h; (k) (i) $(COCl)_2$, toluene, 70 °C, 14 h, (ii) NaN_3, acetone, rt, 2 h, (iii) I_2, 1, 2-dichlorbenzol, reflux, 2.5 h; (l) R-Br, NaH, DMF, 80 °C, 4 h; (m) $LiAlH_4$, $AlCl_3$, THF, rt, 4 h; (n) $LiAlH_4$, THF, rt, 48 h, quench, MeOH/H_2O (100:1), rt.

CHEMISTRY

For the preparation of compounds **9**–**11**, the procedure described in Chuang et al.[16] was used for **9** and modified for **10** and **11** (Scheme 1). Increasing the size of the E ring was found to disfavor ring formation, but the synthesis of **9c** was nevertheless achieved using the same route as for 7-methoxycryptopleurine **9b**, albeit in a lower yield. Reduction of **8** to give **9** was accomplished using sodium bis(2-methoxyethoxy) aluminum hydride in dioxane, but these conditions were not effective in the reduction of **7** to **10** and **11**. After experimentation, it was found that lithium aluminum hydride ($LiAlH_4$) alone or in combination with aluminum chloride ($AlCl_3$) was able to achieve this transformation. The use of $LiAlH_4$ resulted in generation of products **10** (2–11% yields) and **11** (5–25% yields), whereas $LiAlH_4$ in combination with $AlCl_3$ greatly favored product **10** over **11** and thus generated high yields for **10** (42–95%) (see Supporting Information Table S1 and Experimental Section).

The route used to synthesize **22a**–**22d** is depicted in Scheme 2A. Nitrocinnamic acids (**14**) were synthesized through a Perkin reaction[17] from commercially available phenylacetic

dx.doi.org/10.1021/jm300705j | J. Med. Chem. 2012, 55, 10363–10377

acids (**12**) and substituted *o*-nitrobenzaldehydes (**13**). Reduction of the nitro group of **14** afforded aminocinnamic acids (**15**). Phenanthrene acids (**16**) were obtained through a Pschorr cyclization[17] from **15**. Reduction of **16** with diborane in THF afforded **22a**–**22d**.[18] The route shown in Scheme 2B was followed as previously described[19,20] to achieve the synthesis of **22e**. Oxidation of phenanthrene alcohols (**22a**–**22e**) with pyridinium chlorochromate in CH_2Cl_2 afforded the target intermediate phenanthrene aldehydes (**23a**–**23e**).[21] Subsequently, aldehydes (**23**) were converted to isoquinolinones (**28**–**33**) with a modification of a procedure reported by Chuang et al.[16] (Scheme 2C). Reduction of **27** with $LiAlH_4$ in THF at room temperature for 48 h afforded dibenzoisoquinolines **28**–**32** in 13–29% and **33** in 14–31% yields, respectively. This reaction was also greatly improved by reducing **27** with $LiAlH_4$ and $AlCl_3$ (3:1 ratio) in THF at room temperature for 4 h to afford high yields of dibenzoquinolines **28**–**32** (40–80%). The position of hydroxylation was further confirmed by 2D-NMR analyses (Figure 2).

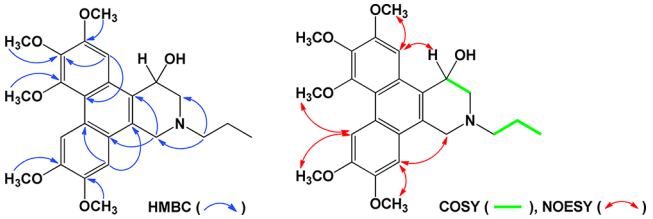

Figure 2. Key COSY, NOESY, and HMBC correlations of **33a**.

RESULTS AND DISCUSSION

Of the tylophorine cyclized E ring analogues synthesized, the quinolizidine **9b** was the most potent inhibitor of cancer cell growth (Table 1), exerting greater activity than indolizidine **9a** by ~2-fold and than **9c** by ~6–8-fold. Similar results were reported for antofine cyclized E ring analogues. This result is consistent with that obtained from the corresponding antofine analogues reported.[22] The same trends of potency for anti-TGEV repliction in ST cells were also found for these compounds (Table 1). Conceivably, an appropriate size and hydrogen atom projection of the E ring optimized the potency of these compounds.

Considering the *N*-alkyl substituent analogues formed by uncyclizing the tylophorine E ring, the propyl **10b** analogue is the most potent compound when compared to ethyl, butyl, and pentyl analogues **10a**, **10c**, and **10d**. When compared to the uncyclized B ring analogues,[3] e.g., septicine (**2** in Figure 1 and Table 1), the uncyclized E ring analogues retained most of the tylophorine activity (Tables 1 and 2), e.g., **2** and **10b** compared to **9a**. Of the branch analogues, in general, the branched methyl group at C1- or C2-position of alkyl substitution slightly or moderately increased the potency of these compounds. For example, isobutyl **10f** and *sec*-butyl **10g** were more potent than butyl **10c** by ~2–6-fold (Table 2). However, the introduction of polar hydroxyl and amine groups to the propyl alcohol **10′m** and propylamine **10′n** decreased their potency dramatically by ~10–30-fold. Further replacement of heterocycle groups for the *N*-substituents, e.g., 3-cyclohexene (**10h**), 2-methyl-[1,3]-dioxolane (**10i**), 2-ethyl-[1,3]dioxolane (**10j**), and 2-propoxytetrahydro-2*H*-pyranyl group (**10k**) also failed to improve potency compared to the alkyl-replaced analogues (Table 2).

Further investigation of the methoxy substituents in the phenanthrene moiety of **10a** and **10b** was also carried out. Of these analogues, **29a** and **29b**, which were demethoxylated at position C2, were found to be more potent than **10a** and **10b**. Thus, the demethoxylation at C2 of phenanthrene moiety improved the activity of the uncyclized E-ring tylophorine analogues. However, the demethoxylation at the positions of 6 or 7 to give **30a**, **30b**, **31**, and **32** dramatically weakened the potency. Methoxylation at C4 did not affect the potency significantly when comparing the activities of **28a** to **10a**, **28b** to **10b**, **28c** to **10c**, and **28d** to **10e** (Table 3). Further introduction of a hydroxyl group to C14 of the C4 demethoxylated compounds with a *N*-alkyl group (Table 4) increased the potency by ~3–6-fold for **11a** compared to **10a**, by ~9–20-fold for **33b** compared to **29a**, by ~4–9-fold for **33c** compared to **29b**, and by ~2-fold for **33d** compared to **29c**. However introduction of a hydroxyl group to the same position C14 of other compounds did not show same tendency for improving activity, e.g., no significant improvement observed for **33a** compared to **28b**; decreased potency occurred to **11b**

Table 1. The Effect of the E Ring Size and *seco*-Structure of Tylophorine Derivatives on the Anti-TGEV in ST Cells and Antiproliferative Activities against Carcinoma Cells

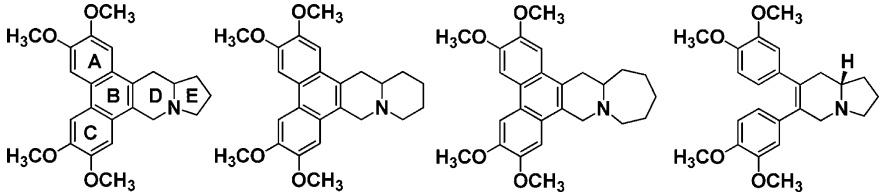

	GI_{50} (μM)[a]					EC_{50} (μM)[a]
compd ID	NCI-H460	MCF7	SF268	HONE-1	NUGC-3	TGEV
9a	0.23	0.24	0.27	0.27	0.19	0.08
9b	0.10	0.11	0.14	0.14	0.14	0.03
9c	0.93	0.96	0.96	1.15	0.62	1.05
2[b]	17.0	18.5	24.2	17.3	14.5	15.4

[a] GI_{50} and EC_{50} values expressed in μM as the mean values of at least three experiments each in duplicate. Values of SD were less than 30% of GI_{50} and EC_{50} values and data not shown. [b] (+)-*S*-Septicine isolated from *Tylophora ovata*.[3]

dx.doi.org/10.1021/jm300705j | *J. Med. Chem.* 2012, 55, 10363–10377

Table 2. Anti-TGEV in ST Cells and Antiproliferative Activity against Carcinoma Cells of Tylophorine-Derived Dibenzoquinolines with a Variety of *N*-Substituents

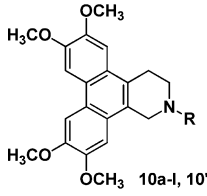

10a-l, 10'm, 10'n

compd		GI_{50} (μM)[a]						EC_{50} (μM)[a]
ID	R	NCI-H460	MCF7	HepG2	HONE-1	NUGC-3	A549	TGEV-IFA
10a	CH_2CH_3	1.01	0.75	1.00	1.57	0.62	0.97	1.65
10b	$(CH_2)_2CH_3$	0.45	0.51	0.77	1.21	0.47	0.73	0.83
10c	$(CH_2)_3CH_3$	2.05	1.97	3.04	2.75	1.93	2.22	4.39
10d	$(CH_2)_4CH_3$	6.11	9.51	8.05	6.20	7.67	ND[b]	6.53
10e	$CH(CH_3)_2$	0.29	0.34	0.67	0.94	0.32	0.38	0.60
10f	$CH_2CH(CH_3)_2$	0.87	0.91	1.81	1.72	1.04	1.32	1.36
10g	$CH(CH_3)CH_2CH_3$	0.45	0.40	0.51	1.15	0.44	0.53	0.73
10h	3-cyclohexene	2.30	2.21	3.64	2.53	1.88	1.92	2.99
10i	2-methyl-[1,3]dioxolane	18.52	22.45	41.04	22.06	19.09	31.50	>50.00
10j	2-ethyl-[1,3]dioxolane	4.15	4.60	6.49	6.13	4.95	4.82	31.89
10k	$(CH_2)_3$OTHP	7.49	9.80	13.98	9.65	8.22	3.78	30.84
10l	$(CH_2)_3$NHBoc	2.89	3.35	4.15	4.52	3.40	3.55	1.027
10′m	$(CH_2)_3$OH	9.41	7.14	16.89	16.60	6.63	5.47	19.28
10′n	$(CH_2)_3NH_2$	11.73	15.32	36.93	21.13	10.33	6.04	23.42
paclitaxel[c]		0.03	0.03	0.18	0.02	0.02	0.06	ND[b]

[a]GI_{50} and EC_{50} values expressed in μM as the mean values of at least three experiments each in duplicate. Values of SD were less than 30% of GI_{50} and EC_{50} values and data not shown. [b]ND, not determined. [c]Paclitaxel, a positive control.

Table 3. Anti-TGEV in ST Cells and Antiproliferative Activity against Carcinoma Cells of Tylophorine-Derived Dibenzoquinolines with a Variety of *N*-Substituents

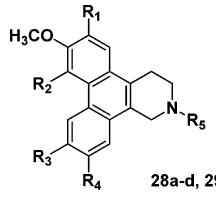

28a-d, 29a-c, 30a-b, 31, 32

	substitution					GI_{50} (μM)[a]						EC_{50} (μM)[a]
compd ID	R1	R2	R3	R4	R5	NCI-H460	MCF7	HepG2	HONE-1	NUGC-3	A549	TGEV-IFA
28a	OCH_3	OCH_3	OCH_3	OCH_3	CH_2CH_3	0.87	1.18	2.50	1.99	1.70	1.41	1.14
28b	OCH_3	OCH_3	OCH_3	OCH_3	$(CH_2)_2CH_3$	0.49	0.62	0.86	0.96	0.54	0.79	0.77
28c	OCH_3	OCH_3	OCH_3	OCH_3	$(CH_2)_3CH_3$	2.68	3.19	5.01	4.06	2.54	3.01	2.92
28d	OCH_3	OCH_3	OCH_3	OCH_3	$CH(CH_3)_2$	0.57	0.72	1.61	1.12	0.64	0.76	0.78
29a	H	H	OCH_3	OCH_3	CH_2CH_3	0.30	0.37	0.66	0.57	0.32	0.40	0.58
29b	H	H	OCH_3	OCH_3	$(CH_2)_2CH_3$	0.26	0.42	0.48	0.77	0.43	0.47	0.68
29c	H	H	OCH_3	OCH_3	$(CH_2)_3CH_3$	3.51	4.73	4.04	4.77	3.99	2.39	5.60
30a	OCH_3	H	H	OCH_3	CH_2CH_3	3.39	3.12	4.01	4.87	3.48	4.38	14.18
30b	OCH_3	H	H	OCH_3	$(CH_2)_2CH_3$	3.82	3.75	4.48	5.56	4.63	4.64	8.91
31	OCH_3	H	OCH_3	H	$(CH_2)_2CH_3$	2.40	2.83	3.17	3.31	2.94	2.95	8.68
32	H	OCH_3	H	OCH_3	$(CH_2)_2CH_3$	3.76	4.11	6.29	4.75	3.72	3.67	2.63

[a]GI_{50} and EC_{50} values expressed in μM as the mean values of at least three experiments each in duplicate. Values of SD were less than 30% of GI_{50} and EC_{50} values and data not shown.

and **11c** compared to **10b** and **10e**, respectively, by a factor of ~2−4. Thus, only the introduction of C14 hydroxyl group to **29a** (a demethoxylated dibenzoquinoline at C2 and C4) synergized the effect of demethoxylation at C2 to give the most potent dibenzoquinoline **33b**. Demethoxylation at C2 may allow the C14 hydroxyl group to participate in an important bonding interaction in the target binding pocket, giving rise to the significantly improved potency.

The dibenzoquinolines assayed above for anticancer cell growth also were tested for anti-TGEV (Tables 2−4) and anti-inflammatory activity (Table 5) in vitro and found to exert the same trends of potency in these three different biological actvities. In addition, the cellular activities which were reported

dx.doi.org/10.1021/jm300705j | J. Med. Chem. 2012, 55, 10363−10377

Table 4. Anti-TGEV in ST Cells and Antiproliferative Activities against Carcinoma Cells of Tylophorine-Derived Dibenzoquinolines with a Hydroxyl Group at the C14 Position

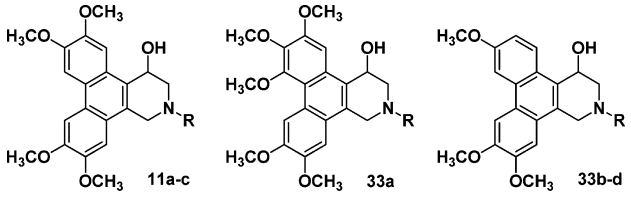

compd		GI_{50} (μM)[a]						EC_{50} (μM)[a]
ID	R	NCI-H460	MCF7	HepG2	HONE-1	NUGC-3	A549	TGEV-IFA
11a	CH_2CH_3	0.17	0.16	0.36	0.44	0.15	0.19	0.34
11b	$(CH_2)_2CH_3$	1.08	1.02	1.68	1.74	0.73	1.19	0.67
11c	$CH(CH_3)_2$	1.07	1.21	1.86	1.71	0.87	1.23	2.74
33a	$(CH_2)_2CH_3$	0.59	0.59	0.83	0.82	0.49	0.82	0.66
33b	CH_2CH_3	0.02	0.04	0.04	0.06	0.03	0.02	0.04
33c	$(CH_2)_2CH_3$	0.05	0.11	0.11	0.14	0.11	0.05	0.12
33d	$(CH_2)_3CH_3$	1.48	2.33	1.85	3.00	1.86	1.32	2.92

[a] GI_{50} and EC_{50} values expressed in μM as the mean values of at least three experiments each in duplicate. SD values were less than 30% of GI_{50} and EC_{50} and data not shown.

Table 5. Anti-inflammatory Activity of Tylophorine Derived Dibenzoquinolines in Terms of Suppression Nitric Oxide Production in LPS/IFNγ Stimulated RAW264.7 Cells

	Raw 264.7/LPS + IFNγ	
compd ID	EC_{50} (μM)[a]	CC_{50} (μM)[a]
9a	0.27	1.24
10a	1.42	>4.0
10b	1.38	>4.0
10e	0.86	>4.0
11a	0.38	>2.0
11b	2.20	>4.0
11c	2.05	>4.0
33b	0.07	0.24

[a] EC_{50} and CC_{50} values expressed in μM as the mean values of at least three experiments each in duplicate. SD values were less than 30% of EC_{50} and CC_{50} and data not shown. EC_{50} was measured for the effective concentration for 50% inhibition of the compound treatment on the production of nitric oxide. CC_{50} was measured for the concentration of 50% inhibition of the compound treatment on the cell growth to distinguish the potency and cytotoxicity.

to account for modes of actions exerted by tylophorine in these three biological systems[5,8,23,24] were also examined for these dibenzoquinolines. These compounds down-regulated the cyclin A2 expression and caused the accumulation of c-Jun in carcinoma cells (Figure 3A and Supporting Information S1A), inhibited iNOS and COX-2 protein expression in LPS/IFNγ stimulated RAW264.7 cells (Figure 3B and Supporting Information Figure S1B), and exerted anti-TGEV nucleocapsid (N) protein expression and TGEV induced apoptosis through inhibition of the activation of caspase 3 from cleavage of procaspase 3 in ST cells (Figure 3C,D and Supporting Information Figure S1C). Thus, these compounds likely retain the same modes of actions as tylophorine.[5,8,23] In the three biological systems tested above, synthesis of RNA or protein are largely in demand, e.g., for cancer cell proliferation, viral replication, or production of proinflammatory factors. Common properties might be shared by the direct molecular targets of these compounds in the three biological systems, e.g., interfering in RNA or protein synthesis. Elucidation of the direct targets of these compounds and their fundamental mechanisms of action is under investigation in our laboratory.

These compounds also potently inhibited the cytopathic effect induced by murine hepatitis virus in DBT cells (Figure 4 and Supporting Information Figure S2). Solubility testing found them to be ~4−5-fold more soluble in DMSO (Table 6) and in DMA (data not shown), compared to their respective related pentacyclic compounds, e.g., **10b** vs **9a** and **10c** vs **9b**. For comparison of **33a** to tylophorine **9a**, ~6-fold increase was found. This improvement gave the guide for the formula choice of in vivo tests followed.

On the basis of these results, **10b**, **29a**, and **33b** were selected for in vivo evaluation. Efficacy tests using paw edema and tumor xenograft murine models, as well as pharmacokinetic tests, were conducted. For the pharmacokinetic studies, compounds were administered to rats intravenously and orally each at 3 mg/kg body weight. Blood samples were taken and the plasma analyzed. It was found that **9a** and **9b** exhibited oral bioavailabilities of 66% and 53%, as described.[8] Tylophovatine C isolated from *T. ovata*[3] was tested and analyzed in parallel as a reference C14-hydroxytylophorine derivative. Pharmacokinetic parameters were also obtained (Table 7). Tylophovatine C, **10b**, **29a**, and **33b** all exhibited good oral bioavailabilities of 54%, 63%, 105%, and 64%, respectively.

In an A549 xenografted tumor mouse model, **33b** significantly and effectively reduced the tumor volume at the dose of 10 mg/kg (oral administration) and resulted in a 61% volume reduction by the end of the test. This is the first report of an antitumor tylophorine-derived compound, orally active in vivo. There were no signs of overt toxicity during the course of the experiment (Figure 5A). In the rat paw edema model, intraperitoneal administration of **33b** resulted in significant inhibition of acute inflammation by reducing the paw edema volume greater than 60% at doses of 3 and 5 mg/kg body weight, respectively (Figure 5B). The neurotoxicity of **33b** was examined by a rota-rod test for motor coordination[25] for three consecutive days. No adverse effect on motor coordination was observed from the **33b** treated groups when compared to the control vehicle and nontumor-bearing groups. Nontheless, the group of **33b** at the dose 10 mg/kg on the day 3 was found to have better coordination than those from the nontumor-

dx.doi.org/10.1021/jm300705j | J. Med. Chem. 2012, 55, 10363−10377

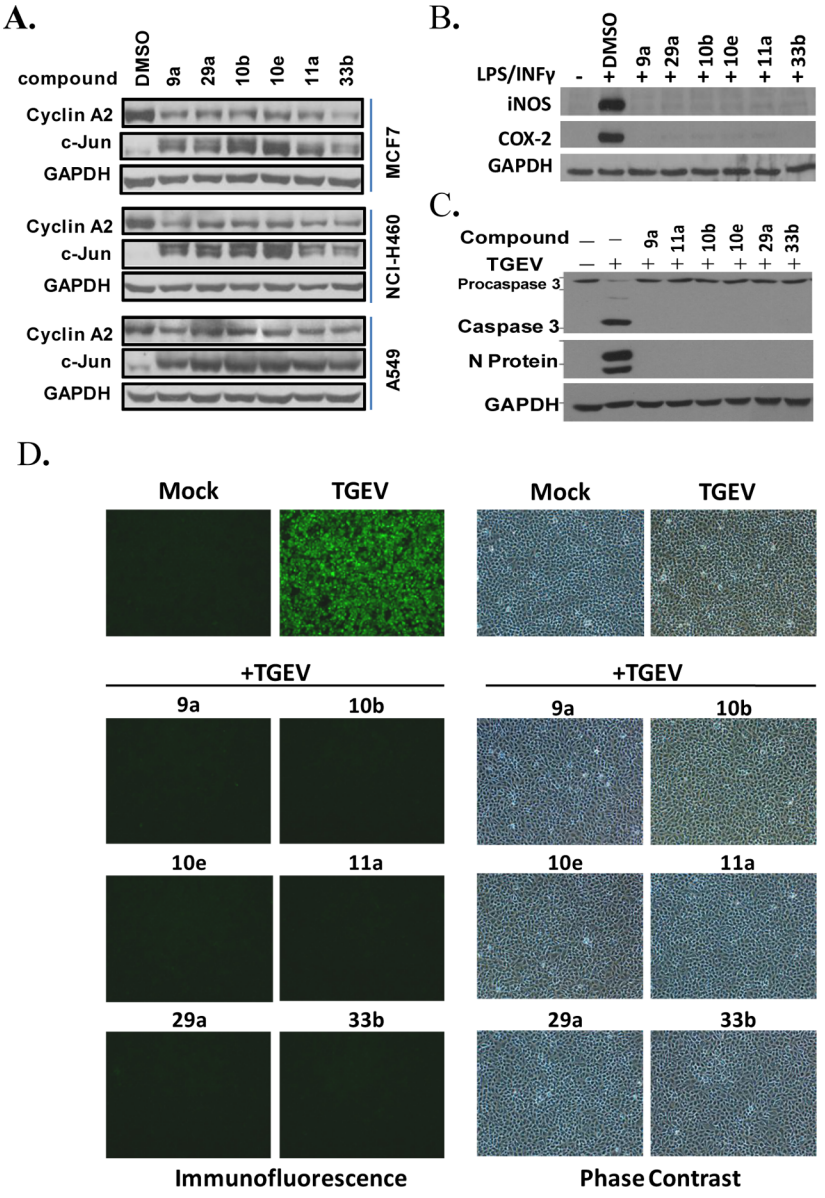

Figure 3. Pharmacological activities of tylophorine and tylophorine-derived dibenzoquinolines in three biological systems. (A) Western analysis for expression of cyclin A2 and c-Jun in carcinoma cells after compound treatment for 24 h. Tylophorine compounds down-regulated cyclin A2 expression and induced c-Jun protein accumulation to exert their anticancer effect. (B) Western analysis for iNOS, COX-2, and GAPDH protein expression in LPS/INFγ stimulated RAW264.7 cells after compound treatment for 20 h. Tylophorine compounds inhibited the induction of iNOS and COX-2 expression in LPS/INFγ stimulated RAW264.7 cells to exert their anti-inflammatory effect. (C) Western analysis for TGEV nucleocapsid (N) protein, caspase 3, and GAPDH in TGEV infected ST cells at 16 hpi. Tylophorine compounds inhibited TGEV N protein expression and activation of caspase 3 through cleavage of pro-casapase 3 to exert their anti-TGEV effect. (D) Immunofluorescent assay for TGEV N and spike protein expression in TGEV infected ST cells at 6 hpi. Phase contrast images were shown for the field of ST cells assayed. (C) and (D) are for anti-TGEV effect. The concentrations of treatment used for all the above experiments are 2 μM for **9a**, **29a**, and **11a**, 4 μM for **10b** and **10e**, and 0.5 μM for **33b**. The results shown are representative of at least three independent experiments.

bearing group with a $*p$ value of <0.001 (Figure 5C). Therefore, **33b** was suggested to be an orally active agent not only effective against tumors without neurotoxicity but also of potential utility for treating inflammatory related diseases and coronaviral infections.

CONCLUSION

A series of tylophorine derived dibenzoquinolines has been synthesized and the constituents tested for anticancer, anti-inflammatory, and anticoronavirus activity. The most potent compound dibenzoquinoline **33b** showed: (1) improved solubility compared to tylophorine **9a**, (2) in vivo efficacies in an A549 xenografted mouse model and a murine paw edema model, when administrated orally and intraperitoneally respectively, (3) good bioavailability, and (4) no measurable neurotoxicity as tested by a rota-rod test for motor coordination. To the best of our knowledge, dibenzoquinoline **33b** is the first example of an orally active tylophorine related compound. By uncyclizing the tylophorine E ring, a new class of compounds has been revealed which may prove useful for improving solubility and potency and diminishing the neurotoxicity of tylophorine derived compounds in the future.

dx.doi.org/10.1021/jm300705j | J. Med. Chem. 2012, 55, 10363−10377

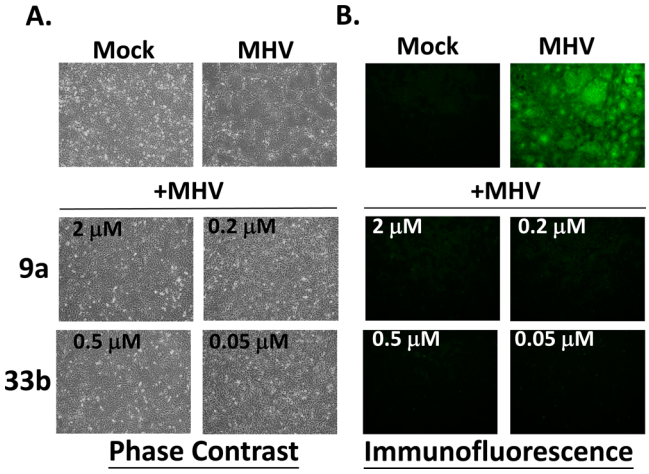

Figure 4. Tylophorine **9a** and dibenzoquinolines **33b** exerted activities for anti-MHV induced cytopathic effect and antiviral protein expression in infected DBT cells. (A) Phase contrast images were shown for cytopathic effect in MHV infected DBT cells at 24 hpi. (B) Immunofluorescent assay for MHV N protein expression in MHV infected DBT cells at 24 hpi. Compound concentrations used as indicated. The results shown are representative of at least three independent experiments.

Table 6. Solubility of Tylophorine-Related Compounds in DMSO

solubility compd	mM	mg/mL
9a	10.0	3.9
9b	12.3	5.0
10a	50.0	18.3
10b	50.0	19.8
10c	45.0	18.4
33b	60.5	22.2

EXPERIMENTAL SECTION

Chemistry. Reagents and all solvents were analytically pure and used without further purification. All reactions were carried out in oven-dried flasks with magnetic stirring. Column chromatography was done using silica gel (Merck Kieselgel 60, no. 9385, 230−400 mesh ASTM). Reactions were monitored with thin-layer chromatography (TLC) using Merck 60 F254 silica gel glass-backed plates and visualized under UV (254 nm). Melting points were measured with a Yanaco micromelting point apparatus (MP-500D). Nuclear magnetic resonance (^{1}H and ^{13}C NMR) spectra were recorded on Varian 300 or 400 or Varian Inova-600 spectrometers in δ (ppm) referenced to tetramethylsilane. Proton coupling patterns were described as singlet (s), doublet (d), triplet (t), multiplet (m), and broad (br). Low resolution mass spectra (LRMS) were given with electric, electrospray, and atmospheric pressure chemical ionization (EI, ESI, and APCI) produced by a Finnigan MAT 95XL, Agilent 1100 series, and Agilent 1200 series. High resolution mass spectra (HRMS) were given with electric ionization (EI) produced by a Finnigan MAT 95XL. Preparative high pressure liquid chromatography (HPLC) was performed using a JASCO model PU-2087 HPLC system equipped with a JASCO model UV-2075 detector and a Thermo hypersil silica column (5 μm, 10 mm × 250 mm). Purities of the target compounds were initially confirmed by less than two degrees interval of melting point, TLC, and HRMS and subsequently determined using a Hitachi 2000 series HPLC system with a reverse phase C18 column (Agilent ZORBAX Eclipse XDB-C18: 5 μm, 4.6 mm × 150 mm, 0.5 mL/min flow rate). Mobile phase A was acetonitrile. Mobile phase B was 10 mM NH_4OAc aqueous solution containing 0.1% formic acid. The gradient system started from A/B (10%:90%) at 0 min to A/B (90%:10%) at 45 min. All compounds tested in the biological assay

Table 7. Pharmacokinetic Properties of Tylophorine-Derived Dibenzoquinolines in Rats

	IV					PO				
compd	dose(mg/kg)	$T_{1/2}$[a] (h)	CL (mL/min/kg)	V_{ss} (L/kg)	$AUC_{(0-inf)}$ (ng/mL· h)	dose (mg/kg)	$T_{1/2}$ (h)	C_{max} (ng/mL)	T_{max} (h)	$AUC_{(0-inf)}$ (ng/mL· h)	F[c] (%)
10b	3	2.7 ± 0.2[b]	60.8 ± 4.5	9.0 ± 0.1	824 ± 66	3	2.4 ± 0.6	87 ± 44	4 ± 2	515 ± 162	62.8
29a	3	16.0 ± 10.6	20.0 ± 9.1	5.1 ± 3.8	2321 ± 658	3	6.3 ± 0.6	535 ± 282	0.3 ± 0	2467 ± 1965	105
33b	3	0.8 ± 0.1	51.8 ± 7.0	2.7 ± 0.5	999 ± 139	3	11.8 ± 5.9	72.4 ± 30.9	0.3 ± 0	646 ± 425	63.5
tylophovatine C	1.5	4.6 ± 0.2	37.6 ± 8.3	12.4 ± 2.7	448 ± 58	1.5	7.6 ± 4.3	39 ± 2	4.3 ± 3.5	453 ± 11	54.3

[a] $t_{1/2}$, apparent elimination half-life; V_{ss}, volume of distribution at steady state; C_{max}, maximal concentration; $AUC_{(0-inf)}$, area under concentration curve from time 0 to infinity. [b] Data are mean values ± SD. [c] F, bioavailability. Administration routes, intravenous (iv) and oral (po).

dx.doi.org/10.1021/jm300705j | J. Med. Chem. 2012, 55, 10363−10377

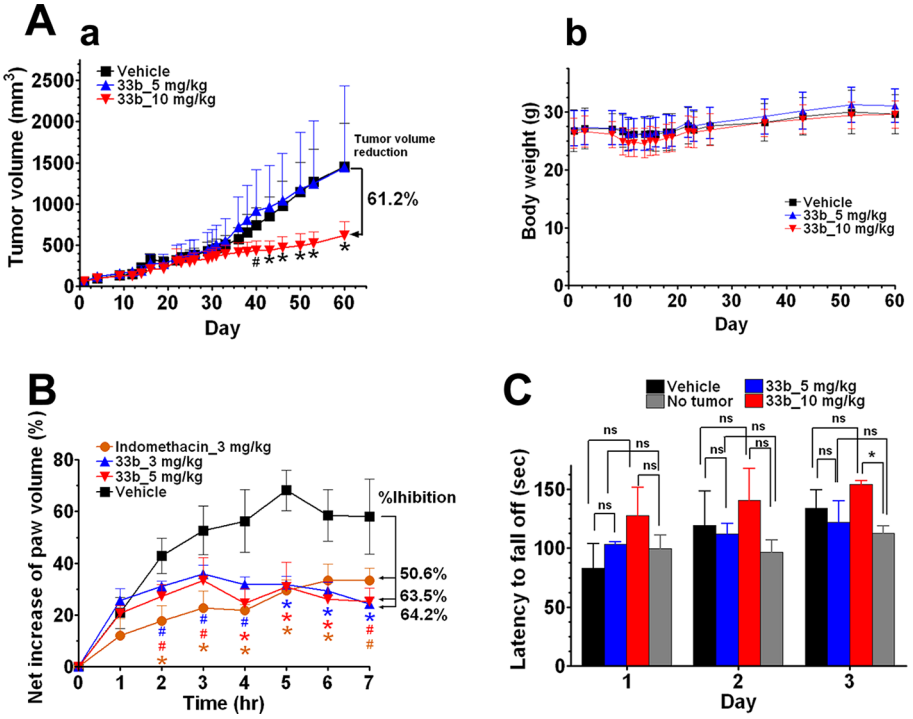

Figure 5. In vivo efficacies of **33b**. (A(a)) Tumor growth curves in NU/NU mice treated with **33b** using a lung A549 xenograft model. (A(b)) Body weight curves in NU/NU mice treated with **33b**. (B) Anti-inflammatory effect in Sprague–Dawley rats treated with **33b** and indomethacin using a murine paw edema model. (C) Neurotoxicity determination by a rota-rod test for motor coordination of NU/NU mice treated with **33b**. $^{*}p < 0.001$; $^{\#}p < 0.01$; ns, no significance; bar, SD.

showed >95% purity at 254 nm except 87.8% for **10′n**, which could not be purified further (see Supporting Information Table S2).

Solubility Determination in DMSO. Saturation concentrations for solubility of the test compounds in DMSO were determined by dissolving compounds in DMSO with assistance of sonication and the maximal volume before compound precipitation occurred was measured for calculation of solubility.

*General Procedure for the Preparation of **14a–c** and **19**.* 6-Nitroveratraldehyde (5 g, 23.7 mmol) and homoanisic acid (3.93 g, 23.7 mmol) were dissolved in acetic anhydride (20 mL), and then triethylamine (3.3 mL) was added slowly. The resultant solution was stirred at 90 °C for 15 h. At this point, H_2O (2 mL) was added and the reaction was allowed to continue for 15 min. After, K_2CO_3 (26 g) in water (240 mL) was added slowly and the mixture was stirred for 60 °C for 1 h. The reaction mixture was cooled to 4 °C and acidified with 12N HCl. The aqueous solution was extracted with CH_2Cl_2, and the obtained organic phases were combined, washed with brine, dried, and then evaporated. Pure **14a** (6.86 g) was obtained by further crystallization from EtOAc.

*General Procedure for the Preparation of **15a–c**.* A solution of 25% NH_4OH (40 mL) was degassed with nitrogen for 30 min and heated to 100 °C before the addition of a $FeSO_4{\cdot}7H_2O$ (15 g, 56 mmol) with stirring. A solution of the nitrocinnamic acid **14a** (2 g, 5.6 mmol) in 70 mL of 25% NH_4OH was added slowly to the reaction mixture, under nitrogen at 100 °C for 2 h. After reaction was completed, the reaction mixture was cooled to room temperature to add decolorizing carbon and then the mixture was filtered. The filtrate was cooled to 4 °C, acidified to pH 3 with 85% H_3PO_4, and extracted with $CHC1_3$/2-propanol (3:1 v/v), washed with water, dried, and evaporated to give the aminocinnamic acid **15a** (1.51 g).

*General Procedure for the Preparation of **16a–d**.* The aminocinnamic acid **15a** (1.51 g, 4.6 mmol) was dissolved in acetone (250 mL) before subsequent slow additions of H_2SO_4 (0.5 mL, 9.2 mmol) and isoamyl nitrite (1.23 mL, 9.2 mmol) at 4 °C. In those cases where a precipitate was still present after 30 min of stirring, water was added until the solution became homogeneous. After 1 h, sodium iodide (3.6 g, 23.9 mmol) was added in five portions for 5 h. Sodium bisulfite was added to turn the mixture yellow, whereupon it was poured into water (500 mL) and extracted with $CHC1_3$, washed with water, dried, and evaporated to give the phenanthrene acid **16a** (1.07 g).

*General Procedure for the Preparation of **22a–d**.* The hydroboration solvent $BH_3{\cdot}THF$ (1 M, 8.75 mL) was added, in three portions, to a stirred suspension of acid **16a** (910 mg, 2.9 mmol) in THF (29 mL) over 1 h. Upon completion of addition, the reaction mixture was warmed (38 °C) for another hour, quenched (HOAc), and evaporated, and the residue was partitioned between 30 mL portions of CH_2Cl_2 and 10% NaOH. The organic layer was dried, filtered, and evaporated to give the alcohol **22a** (778 mg).

*General Procedure for the Preparation of **20**.* Compound **19** (4.03 g, 12.8 mmol) was dissolved in 77 mL of MeOH containing 5.2 mL of concentrated H_2SO_4, and the mixture was refluxed for 4 h. The solvent was evaporated under reduced pressure, and the residue was partitioned between portions of CH_2Cl_2 and saturated $NaHCO_3$ solution. The organic phase was dried, evaporated, and purified by silica gel column chromatography (EtOAc: hexane = 1:3 v/v) to give **20** (4.06 g).

*General Procedure for the Preparation of **21**.* Anhydrous $FeCl_3$ (6.12 g, 37.8 mmol) was added to a solution of **20** (3.54 g, 10.8 mmol) dissolved in dry CH_2Cl_2 (108 mL) to react at room temperature under nitrogen for 20 h. The reaction solution was then evaporated under reduced pressure and the crude product purified by silica gel column chromatography (EtOAc:hexane = 1:3 v/v) to give **21** (1.88 g).

*General Procedure for the Preparation of **22e**.* A suspension of $LiAlH_4$ (480 mg, 11.6 mmol) in 20 mL of dry THF was added to a solution of **21** (1.88 g, 5.8 mmol) dissolved in 30 mL of dry THF. The reaction mixture was stirred at room temperature under nitrogen for 3 h. The mixture was then quenched by 1.2 mL of H_2O, 1.2 mL of 10% NaOH, and 2.4 mL of H_2O, added sequentially. The mixture was filtered, and the filtrate was evaporated under reduced pressure. The residue was dissolved in $CHC1_3$, and the solution was washed with brine and dried over $MgSO_4$. The combined organic phase was evaporated under reduced pressure. The residue was purified by silica gel column chromatography (EtOAc:hexane = 1:1 v/v) to give alcohol **22e** (1.52 g).

dx.doi.org/10.1021/jm300705j | J. Med. Chem. 2012, 55, 10363–10377

*General Procedure for the Preparation of **23a–e**.* Phenanthrene alcohol **22a** (835 mg, 2.8 mmol) dissolved in 75 mL of dry CH_2Cl_2 was added to a suspension of pyridinium chlorochromate (903 mg, 4.2 mmol) in 10 mL of dry CH_2Cl_2 at 0 °C. The reaction mixture was stirred at room temperature under nitrogen for 2 h. The mixture was diluted with 80 mL of ether and filtered. The solids were washed with $CHC1_3$, and the combined organic phase was concentrated by evaporation under reduced pressure. The residue was purified by silica gel column chromatography (CH_2Cl_2) to give the aldehyde **23a** (726 mg).

*General Procedure for the Preparation of **24a–e**.* A mixture of **23a** (0.73 g, 2.5 mmol) and (carboethoxymethylene)-triphenylphosphorane (1.2 g, 3.4 mmol) in 20 mL of toluene was refluxed under nitrogen for 4 h. After cooling, the resulting solution was directly purified by silica gel column chromatography (CH_2Cl_2) to afford the ethyl ester **24a** (0.89 g).

*General Procedure for the Preparation of **25a–e**.* A solution of 8 mL of 1 N KOH was added to a solution of the ester **24a** (0.81 g, 2.2 mmol) in 16 mL of EtOH, and the reaction mixture was heated to reflux for 3 h. After cooling, the reaction solution was evaporated and the residue was dissolved in 16 mL water, acidified with 10% HCl, and extracted with 70 mL of $CHCl_3$ and 60 mL of EtOAc. The combined extracts were dried with anhydrous $MgSO_4$, filtered, and evaporated under reduced pressure to give the acrylic acid **25a** (0.73 g)

*General Procedure for the Preparation of **26a–e**.* A mixture of **25a** (1.26 g, 3.7 mmol) and oxalyl chloride (1.89 g, 14.8 mmol) in 63 mL of toluene was heated for 15 h at 70 °C. After cooling, the resulting mixture was concentrated under reduced pressure to afford the acyl chloride. The acyl chloride was added immediately to a suspension of NaN_3 (0.73 g, 11.1 mmol) in 120 mL of dry acetone in an ice bath. The reaction mixture was stirred for 2 h at room temperature and filtered. The solvent was evaporated under reduced pressure, and the residue was purified by silica gel column chromatography ($CHCl_3$) to afford acryloyl azide. A mixture of azide and I_2 (0.02 g, catalytic amount) in 18 mL of *o*-dichlorobenzene was refluxed for 2 h. After cooling, compound **26a** was isolated by filtration and washed with CH_2Cl_2 to afford pure isoquinolinone **26a** (1.01 g)

*General Procedure for the Preparation of **7a–l** and **27a–k**.* A suspension of NaH (60% dispersion in oil, 119 mg, 2.98 mmol) in 1 mL of DMF cooled in an ice bath was added to a solution of **26a** (400 mg, 1.2 mmol) in 15 mL of DMF with stirring at room temperature under nitrogen for 30 min. After the addition was completed, the mixture was added slowly to a solution of bromoethane (4.77 mmol) in 1 mL of DMF. The mixture was stirred at 80 °C for 4 h. The solvent was evaporated under reduced pressure, and water was then added. The mixture was extracted with CH_2Cl_2, dried over $MgSO_4$, and concentrated under reduced pressure. The residue was purified by silica gel column chromatography (EtOAc:CH_2Cl_2 = 1:8 v/v) to afford the alkyll isoquinolinone of **27a** (400 mg).

*General Procedure for the Preparation of **10a–n**, **11a–c**, **28a–d**, **29a–c**, **30a–b**, **31**, **32**, and **33a–d**. 1. Reduction by $LiAlH_4$ and $AlCl_3$ for Method d in Scheme 1 and Method m in Scheme 2.* A solution of $AlCl_3$ (18 mg, 0.13 mmol) in 0.5 mL of dry THF was added to a stirred suspension of **27a** (48 mg, 0.13 mmol) in 2 mL of dry THF cooled at −15 °C. The mixture was stirred at room temperature under nitrogen for 15 min, and then $LiAlH_4$ (26 mg, 0.65 mmol) was added at −15 °C. The reaction mixture was warmed up to room temperature for 4 h and then quenched by 5 mL of MeOH, and 5 mL of 10% NaOH sequentially. The mixture was filtered, and the filtrate was evaporated under reduced pressure. The residue was purified by silica gel column chromatography (MeOH:EtOAc:CH_2Cl_2 = 1:10:20 v/v) to afford the dibenzo[*f*,*h*]isoquinolinone of **29a** (19 mg).

2. Reduction by $LiAlH_4$ for Method e in Scheme 1 and Method n in Scheme 2. A solution of $LiAlH_4$ (136 mg, 3.58 mmol) in 5 mL of dry THF was added to a stirred suspension of **27a** (100 mg, 0.28 mmol) in 8 mL of dry THF cooled at −15 °C,. The reaction mixture was warmed up to room temperature for 2 days, then 5.5 mL of MeOH/H_2O (100:1) was added slowly using a syringe pump. The mixture was filtered, and the filtrate was evaporated under reduced pressure. The residue was purified by silica gel column chromatography (MeOH:EtOAc:CH_2Cl_2 = 0:10:20, 1:10:20, 2:10:20; all solvent with 0.001% diethylamine) to afford the **29a** and **33b** mixtures. The mixtures were further purified by HPLC (5 μm, 10 mm × 250 mm; MeOH:EtOAc:CH_2Cl_2 = 1:10:20, 2:10:20; all solvent with 0.001% diethylamine) at 1 mL/min flow rate to afford **29a** (15 mg) and **33b** (31 mg).

*2-Ethyl-6,7,10,11-tetramethoxy-1,2,3,4-tetrahydrodibenzo[f,h]-isoquinoline (**10a**).* Yield 9% (method e); white crystal; mp 186 °C. ^{1}H NMR (400 MHz, $CDCl_3$): 1.31 (t, J = 7.2 Hz, 3H), 2.81 (quartet, J = 7.2 Hz, 2H), 2.96 (t, J = 5.6 Hz, 2H), 3.22 (t, J = 5.6 Hz, 2H), 4.02 (s, 2H), 4.04 (s, 3H), 4.05 (s, 3H), 4.12 (s, 6H), 7.15 (s, 1H), 7.29 (s, 1H), 7.82 (s, 1H), 7.83 (s, 1H). ^{13}C NMR (75 MHz, $CDCl_3$): 12.2, 26.7, 49.4, 52.0, 53.4, 55.8, 55.9, 56.9, 102.8, 103.3, 103.4, 103.8, 123.4, 123.5, 124.1, 124.7, 125.5, 125.6, 148.4, 148.5, 148.7. MS (EI) m/z 381 (M^+, 100%). HRMS calcd for $C_{23}H_{27}NO_4$ (M^+) 381.1940; found 381.1930.

*6,7,10,11-Tetramethoxy-2-propyl-1,2,3,4-tetrahydrodibenzo[f,h]-isoquinoline (**10b**).* Yield 76% (method d), 7% (method e); white crystal; mp 176–178 °C. ^{1}H NMR (400 MHz, $CDCl_3$): 1.02 (t, J = 7.6 Hz, 3H), 1.74 (sextet, J = 7.6 Hz, 2H), 2.67 (t, J = 7.6 Hz, 2H), 2.92 (t, J = 6.0 Hz, 2H), 3.18 (t, J = 6.0 Hz, 2H), 3.98 (s, 2H), 4.03 (s, 3H), 4.04 (s, 3H), 4.10 (s, 6H), 7.12 (s, 1H), 7.27 (s, 1H), 7.79 (s, 1H), 7.80 (s, 1H). ^{13}C NMR (100 MHz, $CDCl_3$): 12.0, 20.5, 27.2, 50.1, 54.3, 55.8, 55.9, 56.0, 60.6, 102.9, 103.2, 103.4, 103.8, 123.3, 123.4, 124.3, 125.6, 125.9, 148.3, 148.4, 148.6. MS (EI) m/z 395 (M^+, 100%). HRMS calcd for $C_{24}H_{29}NO_4$ (M^+) 395.2097; found 395.2098.

*2-Butyl-6,7,10,11-tetramethoxy-1,2,3,4-tetrahydrodibenzo[f,h]-isoquinoline (**10c**).* Yield 66% (method d); white needle; mp 172–173 °C. ^{1}H NMR (300 MHz, $CDCl_3$): 1.00 (t, J = 7.5 Hz, 3H), 1.45 (sextet, J = 7.5 Hz, 2H), 1.70 (quintet, J = 7.5 Hz, 2H), 2.70 (t, J = 7.5 Hz, 2H), 2.91 (t, J = 5.7 Hz, 2H), 3.18 (t, J = 5.7 Hz, 2H), 3.97 (s, 2H), 4.03 (s, 3H), 4.04 (s, 3H), 4.10 (s, 6H), 7.12 (s, 1H), 7.26 (s, 1H), 7.79 (s, 1H), 7.80 (s, 1H). ^{13}C NMR (75 MHz, $CDCl_3$): 14.1, 20.8, 27.2, 29.4, 50.1, 54.3, 55.8, 55.9, 58.4, 102.8, 103.2, 103.3, 103.8, 123.3, 123.4, 124.2, 125.6, 125.9, 148.2, 148.3, 148.5, 148.6. MS (EI) m/z 409 (M^+, 100%). HRMS calcd for $C_{25}H_{31}NO_4$ (M^+) 409.2253; found 409.2252.

*6,7,10,11-Tetramethoxy-2-pentyl-1,2,3,4-tetrahydrodibenzo[f,h]-isoquinoline (**10d**).* Yield 5% (method e); white needle. ^{1}H NMR (300 MHz, $CDCl_3$): 0.95 (t, J = 7.2 Hz, 3H), 1.38–1.43 (m, 4H), 1.70–1.73 (m, 2H), 2.71 (t, J = 7.8 Hz, 2H), 2.94 (t, J = 5.4 Hz, 2H), 3.21 (t, J = 5.4 Hz, 2H), 4.01 (s, 2H), 4.04 (s, 3H), 4.05 (s, 3H), 4.12 (s, 6H), 7.16 (s, 1H), 7.30 (s, 1H), 7.83 (s, 1H), 7.84 (s, 1H). MS (APCI) m/z 424.2 $[M + H]^+$.

*2-Isopropyl-6,7,10,11-tetramethoxy-1,2,3,4-tetrahydrodibenzo-[f,h]isoquinoline (**10e**).* Yield 59% (method d), 2% (method e); white needle; mp 185 °C. ^{1}H NMR (300 MHz, $CDCl_3$): 1.26 (d, J = 6.6 Hz, 6H), 2.95 (t, J = 5.7 Hz, 2H), 3.09 (septet, J = 6.6 Hz, 1H), 3.17 (t, J = 5.7 Hz, 2H), 4.03 (s, 3H), 4.04 (s, 3H), 4.08 (s, 2H), 4.10 (s, 6H), 7.13 (s, 1H), 7.27 (s, 1H), 7.80 (s, 1H), 7.81 (s, 1H). ^{13}C NMR (75 MHz, $CDCl_3$): 18.5, 27.8, 45.1, 49.9, 54.1, 55.8, 55.9, 102.9, 103.2, 103.4, 103.8, 123.3, 124.4, 125.7, 126.1, 148.2, 148.3, 148.5. MS (EI) m/z 395 (M^+, 100%). HRMS calcd for $C_{24}H_{29}NO_4$ (M^+) 395.2097; found 395.2103.

*2-Isobutyl-6,7,10,11-tetramethoxy-1,2,3,4-tetrahydrodibenzo-[f,h]isoquinoline (**10f**).* Yield 69% (method d); light-yellow needle; mp 160–161 °C. ^{1}H NMR (300 MHz, $CDCl_3$): 1.02 (d, J = 6.6 Hz, 6H), 2.04 (septet, J = 6.9 Hz, 1H), 2.47 (d, J = 7.5 Hz, 2H), 2.90 (t, J = 6.0 Hz, 2H), 3.18 (t, J = 6.0 Hz, 2H), 3.97 (s, 2H), 4.03 (s, 3H), 4.04 (s, 3H), 4.11 (s, 6H), 7.13 (s, 1H), 7.29 (s, 1H), 7.80 (s, 1H), 7.81 (s, 1H). ^{13}C NMR (75 MHz, $CDCl_3$): 21.0, 25.8, 27.1, 50.2, 54.8, 55.8, 55.9, 56.0, 66.8, 102.9, 103.2, 103.4, 103.8, 123.3, 123.4, 124.3, 125.6, 125.8, 126.0, 148.3, 148.4, 148.6. MS (EI) m/z 409 (M^+, 100%). HRMS calcd for $C_{25}H_{31}NO_4$ (M^+) 409.2253; found 409.2249.

*2-(sec-Butyl)-6,7,10,11-tetramethoxy-1,2,3,4-tetrahydrodibenzo-[f,h]isoquinoline (**10g**).* Yield 95% (method d); light-yellow crystal; mp 157–158 °C. ^{1}H NMR (300 MHz, $CDCl_3$): 1.00 (t, J = 7.5 Hz, 3H), 1.19 (d, J = 6.3 Hz, 3H), 1.42–1.55 (m, 1H), 1.76–1.87 (m,

2H), 2.81−2.90 (m, 1H), 2.93−3.01 (m, 1H), 3.15 (t, J = 5.4 Hz, 2H), 4.03 (s, 3H), 4.04 (s, 3H), 4.08 (s, 2H), 4.10 (s, 6H), 7.13 (s, 1H), 7.27 (s, 1H), 7.78 (s, 1H), 7.80 (s, 1H). ^{13}C NMR (75 MHz, $CDCl_3$): 11.5, 13.8, 26.3, 28.0, 29.6, 44.8, 49.8, 55.8, 55.9, 60.4, 102.9, 103.2, 103.3, 103.8, 123.3, 124.4, 125.8, 126.3, 126.5, 148.2, 148.3, 148.5. MS (EI) m/z 409 (M^+, 31%) and 380 (100%). HRMS calcd for $C_{25}H_{31}NO_4$ (M^+) 409.2253; found 409.2257.

*2-(Cyclohex-2-en-1-yl)-6,7,10,11-tetramethoxy-1,2,3,4-tetrahydrodibenzo[f,h]isoquinoline (**10h**).* Yield 70% (method d); light-yellow crystal; mp 128−129 °C. ^{1}H NMR (400 MHz, $CDCl_3$): 1.62−1.71 (m, 1H), 1.75−1.77 (m, 1H), 1.92−1.94 (m, 1H), 2.02−2.03 (m, 1H), 2.04−2.08 (m, 2H), 2.91−2.96 (m, 1H), 3.04−3.09 (m, 1H), 3.17 (t, J = 5.2 Hz, 2H), 3.63 (br s, 1H), 4.03 (s, 3H), 4.04 (s, 3H), 4.10 (s, 6H), 4.16 (d, J = 6.0 Hz, 2H), 5.86 (d, J = 10.4 Hz, 1H), 5.95 (d, J = 10.4 Hz, 1H), 7.12 (s, 1H), 7.27 (s, 1H), 7.80 (s, 1H), 7.81 (s, 1H). ^{13}C NMR (100 MHz, $CDCl_3$): 21.7, 23.2, 25.4, 28.0, 45.2, 49.9, 55.8, 56.0, 60.0, 103.0, 103.2, 103.4, 103.9, 123.3, 123.4, 124.4, 125.8, 126.2, 126.3, 129.2, 130.6, 148.3, 148.4, 148.6. MS (EI) m/z 433 (M^+, 100%). HRMS calcd for $C_{27}H_{31}NO_4$ (M^+) 433.2253; found 433.2259.

*2-((1,3-Dioxolan-2-yl)methyl)-6,7,10,11-tetramethoxy-1,2,3,4-tetrahydrodibenzo[f,h]isoquinoline (**10i**).* Yield 42% (method d); white needle; mp 182−183 °C. ^{1}H NMR (300 MHz, $CDCl_3$): 2.96 (d, J = 4.2 Hz, 2H), 3.07 (t, J = 5.1 Hz, 2H), 3.19 (t, J = 5.1 Hz, 2H), 3.91 (AA′BB′, 2H), 4.02 (s, 3H), 4.03 (s, 3H), 4.04 (AA′BB′, 2H), 4.10 (s, 6H), 4.12 (s, 2H), 5.21 (t, J = 4.5 Hz, 1H), 7.12 (s, 1H), 7.26 (s, 1H), 7.79 (s, 1H), 7.80 (s, 1H). ^{13}C NMR (75 MHz, $CDCl_3$): 26.9, 51.0, 54.7, 55.8, 55.9, 60.9, 64.9, 102.9, 103.2, 103.3, 103.8, 123.3, 123.4, 124.2, 125.5, 125.7, 148.3, 148.4, 148.6. MS (EI) m/z 439 (M^+, 13%) and 366 (100%). HRMS calcd for $C_{25}H_{29}NO_6$ (M^+) 439.1995; found 439.1987.

*2-(2-(1,3-Dioxolan-2-yl)ethyl)-6,7,10,11-tetramethoxy-1,2,3,4-tetrahydrodibenzo[f,h]isoquinoline (**10j**).* Yield 45% (method d); white crystal; mp 186−187 °C. ^{1}H NMR (300 MHz, $CDCl_3$): 2.10 (td, J = 7.5, 4.5 Hz, 2H), 2.87 (t, J = 7.5 Hz, 2H), 2.94 (t, J = 5.7 Hz, 2H), 3.18 (t, J = 5.7 Hz, 2H), 3.88 (AA′BB′, 2H), 3.99 (s, 2H), 4.02 (AA′BB′, 2H), 4.03 (s, 6H), 4.10 (s, 6H), 5.04 (t, J = 4.8 Hz, 1H), 7.10 (s, 1H), 7.26 (s, 1H), 7.79 (s, 1H), 7.80 (s, 1H). ^{13}C NMR (75 MHz, $CDCl_3$): 27.2, 31.7, 50.1, 53.3, 54.2, 55.8, 55.9, 56.0, 64.9, 102.8, 102.9, 103.2, 103.3, 103.4, 103.8, 123.3, 123.4, 124.2, 125.4, 125.5, 125.8, 148.3, 148.4, 148.6. MS (EI) m/z 453 (M^+, 51%) and 324 (100%). HRMS calcd for $C_{26}H_{31}NO_6$ (M^+) 453.2151; found 453.2141.

*6,7,10,11-Tetramethoxy-2-(3-((tetrahydro-2H-pyran-2-yl)oxy)-propyl)-1,2,3,4-tetrahydrodibenzo[f,h]isoquinoline (**10k**).* Yield 7% (method e); yellow crystal. ^{1}H NMR (400 MHz, $CDCl_3$): 1.46−1.55 (m, 4H), 1.65−1.70 (m, 1H), 1.75−1.81 (m, 1H), 1.97 (quintet, J = 7.2 Hz, 2H), 2.73−2.77 (m, 2H), 2.87 (t, J = 5.6 Hz, 2H), 3.12 (t, J = 5.6 Hz, 2H), 3.41−3.52 (m, 2H), 3.81−3.86 (m, 2H), 3.93 (s, 2H), 3.96 (s, 3H), 3.97 (s, 3H), 4.00 (s, 6H), 4.53−4.55 (m, 1H), 7.06 (s, 1H), 7.20 (s, 1H), 7.73 (s, 1H), 7.74 (s, 1H). MS (EI) m/z 495 (M^+, 9%) and 410 (100%). HRMS calcd for $C_{29}H_{37}NO_6$ (M^+) 495.2621; found 495.2627.

*tert-Butyl (2-(6,7,10,11-Tetramemthoxy-3,4-dihydrodibenzo[f,h]-isoquinolin-2(1H)-yl)ethyl) carbamate (**10l**).* Yield 47% (method d); yellow crystal; mp 123−124 °C. ^{1}H NMR (300 MHz, $CDCl_3$): 1.43 (s, 9H), 2.84 (t, J = 5.7 Hz, 2H), 2.94 (t, J = 5.7 Hz, 2H), 3.19 (t, J = 5.4 Hz, 2H), 3.44 (quartet, J = 5.7 Hz, 2H), 4.00 (s, 2H), 4.04 (s, 6H), 4.11 (s, 6H), 5.20 (br s, 1H), 7.10 (s, 1H), 7.28 (s, 1H), 7.80 (s, 1H), 7.81 (s, 1H). ^{13}C NMR (75 MHz, $CDCl_3$): 27.2, 28.4, 49.9, 54.0, 54.8, 55.8, 55.9, 56.0, 57.1, 102.8, 103.3, 103.4, 103.8, 123.4, 123.5, 124.1, 125.3, 125.5, 125.9, 148.4, 148.6, 148.7. MS (ESI) m/z 497 (M + H)$^+$.

*3-(6,7,10,11-Tetramethoxy-3,4-dihydrodibenzo[f,h]isoquinolin-2(1H)-yl)propan-1-ol (**10′m**).* Yield 93% (method d); white needle. ^{1}H NMR (300 MHz, $CDCl_3$): 1.95 (quintet, J = 5.6 Hz, 2H), 2.99−3.07 (m, 4H), 3.23 (t, J = 5.6 Hz, 2H), 3.90 (t, J = 5.6 Hz, 2H), 4.04 (s, 3H), 4.06 (s, 3H), 4.11 (s, 2H), 4.12 (s, 6H), 7.13 (s, 1H), 7.28 (s, 1H), 7.83 (s, 1H), 7.84 (s, 1H). MS (EI) m/z 411 (M^+, 97%) and 349 (100%). HRMS calcd for $C_{24}H_{29}NO_5$ (M^+) 411.2046; found 411.2043.

*2-(6,7,10,11-Tetramethoxy-3,4-dihydrodibenzo[f,h]isoquinolin-2(1H)-yl)ethanamine (**10′n**).* Yield 71% (method d); colorless rock; mp 161−162 °C. ^{1}H NMR (300 MHz, $CDCl_3$): 2.80 (t, J = 6.0 Hz, 2H), 2.94 (t, J = 6.0 Hz, 2H), 2.99 (t, J = 6.0 Hz, 2H), 3.19 (t, J = 5.7 Hz, 2H), 4.02 (s, 2H), 4.04 (s, 6H), 4.11 (s, 6H), 7.13 (s, 1H), 7.28 (s, 1H), 7.81 (s, 1H), 7.82 (s, 1H). MS (EI) m/z 396 (M^+, 9%) and 349 (100%). HRMS calcd for $C_{23}H_{28}N_2O_4$ (M^+) 396.2049; found 396.2043.

*2-Ethyl-6,7,10,11-tetramethoxy-1,2,3,4-tetrahydrodibenzo[f,h]-isoquinolin-4-ol (**11a**).* Yield 25% (method e); white needle; mp 185 °C. ^{1}H NMR (300 MHz, $CDCl_3$): 1.25 (t, J = 7.2 Hz, 3H), 2.26 (d, J = 11.1 Hz, 1H), 2.47−2.58 (m, 1H), 2.68−2.79 (m, 1H), 3.00 (d, J = 15.6 Hz, 1H), 3.30−3.36 (m, 1H), 3.35 (d, J = 11.1 Hz, 1H), 3.84 (s, 3H), 4.07 (s, 3H), 4.09 (s, 3H), 4.12 (s, 3H), 4.91 (s, 1H), 6.25 (s, 1H), 7.40 (s, 1H), 7.55 (s, 1H), 7.79 (s, 1H). ^{13}C NMR (100 MHz, $CDCl_3$): 11.3, 52.2, 53.3, 55.6, 55.7, 55.8, 57.2, 64.6, 102.5, 102.5, 102.6, 105.1, 122.6, 123.6, 123.9, 125.3, 126.4, 126.6, 147.9, 148.2, 148.4, 148.5. MS (EI) m/z 397 (M^+, 47%) and 340 (100%). HRMS calcd for $C_{23}H_{27}NO_5$ (M^+) 397.1889; found 397.1880.

*6,7,10,11-Tetramethoxy-2-propyl-1,2,3,4-tetrahydrodibenzo[f,h]-isoquinolin-4-ol (**11b**).* Yield 14% (method e); white rock; mp 202 °C. ^{1}H NMR (400 MHz, $CDCl_3$): 1.02 (t, J = 7.2 Hz, 3H), 1.70−1.81 (m, 2H), 2.46 (d, J = 11.6 Hz, 1H), 2.52−2.59 (m, 1H), 2.65−2.71 (m, 1H), 3.28 (d, J = 15.2 Hz, 1H), 3.35 (d, J = 11.6 Hz, 1H), 3.80 (d, J = 15.2 Hz, 1H), 3.95 (s, 3H), 4.08 (s, 3H), 4.11 (s, 3H), 4.13 (s, 3H), 5.03 (s, 1H), 6.67 (s, 1H), 7.60 (s, 1H), 7.68 (s, 1H), 7.76 (s, 1H). ^{13}C NMR (150 MHz, $CDCl_3$): 12.0, 19.7, 54.0, 55.8, 55.9, 56.0, 58.0, 60.4, 64.7, 102.9, 103.0, 104.9, 123.0, 123.8, 124.2, 125.3, 126.7, 127.3, 148.3, 148.5, 148.7, 148.8. MS (EI) m/z 411 (M^+, 50%) and 340 (100%). HRMS calcd for $C_{24}H_{29}NO_5$ (M^+) 411.2046; found 411.2049.

*2-Isopropyl-6,7,10,11-tetramethoxy-1,2,3,4-tetrahydrodibenzo-[f,h]isoquinolin-4-ol (**11c**).* Yield 5% (method e); yellow crystal; mp 170−172 °C. ^{1}H NMR (300 MHz, $CDCl_3$): 1.24−1.28 (m, 6H), 2.68 (d, J = 11.7 Hz, 1H), 3.11−3.17 (m, 1H), 3.31 (d, J = 11.7 Hz, 1H), 3.89 (d, J = 15.3 Hz, 1H), 4.04 (s, 3H), 4.05 (s, 3H), 4.07 (s, 3H), 4.08 (s, 3H), 4.23 (d, J = 15.3 Hz, 1H), 5.14 (s, 1H), 7.12 (s, 1H), 7.70 (s, 1H), 7.79 (s, 1H), 7.81 (s, 1H). ^{13}C NMR (150 MHz, $CDCl_3$): 17.4, 19.5, 50.3, 52.8, 53.9, 55.9, 56.0, 56.1, 64.6, 103.1, 103.2, 103.3, 104.6, 123.6, 123.9, 124.4, 125.4, 127.4, 128.2, 148.6, 148.7, 149.0, 149.1. MS (ESI) m/z 412 (M + H)$^+$.

*2-Ethyl-6,7,8,10,11-pentamethoxy-1,2,3,4-tetrahydrodibenzo-[f,h]isoquinoline (**28a**).* Yield = 29% (method n); yellow rock; mp 199−200 °C. ^{1}H NMR (400 MHz, $CDCl_3$): 1.31 (t, J = 7.2 Hz, 3H), 2.79 (q, J = 7.2 Hz, 2H), 2.93 (t, J = 5.6 Hz, 2H), 3.19 (t, J = 5.6 Hz, 2H), 3.98 (s, 3H), 4.01 (s, 2H), 4.02 (s, 3H), 4.04 (s, 3H), 4.05 (s, 3H), 4.09 (s, 3H), 7.16 (s, 1H), 7.18 (s, 1H), 9.20 (s, 1H). ^{13}C NMR (150 MHz, $CDCl_3$): 10.1, 22.7, 46.9, 49.4, 50.6, 55.7, 55.8, 56.0, 60.6, 61.4, 100.3, 101.7, 108.3, 118.6, 123.1, 123.4, 124.1, 127.0, 143.1, 148.5, 148.8, 151.8, 152.2. MS (EI) m/z 411 (M^+, 100%). HRMS calcd for $C_{24}H_{29}NO_5$ (M^+) 411.2046; found 411.2050.

*6,7,8,10,11-Pentamethoxy-2-propyl-1,2,3,4-tetrahydrodibenzo-[f,h]isoquinoline (**28b**).* Yield 17% (method n); light-yellow crystal; mp 124−125 °C. ^{1}H NMR (300 MHz, $CDCl_3$): 1.03 (t, J = 7.5 Hz, 3H), 1.74 (sextet, J = 7.5 Hz, 2H), 2.68 (t, J = 7.5 Hz, 2H), 2.92 (t, J = 6.0 Hz, 2H), 3.18 (t, J = 6.0 Hz, 2H), 3.98 (s, 3H), 4.00 (s, 2H), 4.02 (s, 3H), 4.04 (s, 3H), 4.05 (s, 3H), 4.09 (s, 3H), 7.16 (s, 1H), 7.18 (s, 1H), 9.19 (s, 1H). ^{13}C NMR (150 MHz, $CDCl_3$): 12.0, 20.2, 27.1, 49.8, 54.0, 55.7, 55.8, 60.0, 60.5, 61.3, 100.4, 102.2, 108.1, 117.8, 123.5, 124.8, 125.6, 126.6, 128.4, 142.1, 148.0, 151.6, 151.7. MS (EI) m/z 425 (M^+, 100%). HRMS calcd for $C_{25}H_{31}NO_5$ (M^+) 425.2202; found 425.2195.

*2-Butyl-6,7,8,10,11-pentamethoxy-1,2,3,4-tetrahydrodibenzo-[f,h]isoquinoline (**28c**).* Yield 16% (method n); light-yellow crystal; mp 120−123 °C. ^{1}H NMR (400 MHz, $CDCl_3$): 1.00 (t, J = 7.6 Hz, 3H), 1.45 (sextet, J = 7.6 Hz, 2H), 1.70 (quintet, J = 7.6 Hz, 2H), 2.71 (t, J = 7.6 Hz, 2H), 2.92 (t, J = 5.6 Hz, 2H), 3.18 (t, J = 5.6 Hz, 2H), 3.98 (s, 3H), 4.00 (s, 2H), 4.02 (s, 3H), 4.05 (s, 3H), 4.06 (s, 3H), 4.09 (s, 3H), 7.16 (s, 1H), 7.18 (s, 1H), 9.19 (s, 1H). MS (ESI) m/z 440 (M + H)$^+$.

*2-Isopropyl-6,7,8,10,11-pentamethoxy-1,2,3,4-tetrahydrodibenzo[f,h]isoquinoline (**28d**).* Yield 13% (method n); light-yellow crystal; mp 195−198 °C. ^{1}H NMR (300 MHz, $CDCl_3$): 1.12 (d, J = 6.3 Hz, 6H), 2.97 (t, J = 5.4 Hz, 2H), 3.11 (septet, J = 6.3 Hz, 1H), 3.18 (t, J = 5.4 Hz, 2H), 3.98 (s, 3H), 4.02 (s, 3H), 4.04 (s, 3H), 4.06 (s, 3H), 4.09 (s, 3H), 4.11 (s, 2H), 7.16 (s, 1H), 7.18 (s, 1H), 9.19 (s, 1H). MS (ESI) m/z 426 $(M + H)^+$.

*2-Ethyl-7,10,11-trimethoxy-1,2,3,4-tetrahydrodibenzo[f,h]isoquinoline (**29a**).* Yield 40% (method m), 16% (method n); yellow crystal; mp 160−161 °C. ^{1}H NMR (300 MHz, $CDCl_3$): 1.32 (t, J = 7.2 Hz, 3H), 2.80 (q, J = 7.2 Hz, 2H), 2.94 (t, J = 5.7 Hz, 2H), 3.25 (t, J = 5.7 Hz, 2H), 4.00 (s, 2H), 4.01 (s, 3H), 4.05 (s, 3H), 4.10 (s, 3H), 7.14 (s, 1H), 7.21 (dd, J = 9.0, 2.6 Hz, 1H), 7.89 (d, J = 2.6 Hz, 1H), 7.90 (s, 1H), 7.92 (d, J = 9.0 Hz, 1H). ^{13}C NMR (150 MHz, $CDCl_3$): 12.0, 20.4, 50.0, 54.0, 55.5, 55.9, 56.0, 60.3, 102.9, 104.0, 104.6, 114.8, 123.3, 125.1, 125.3, 125.5, 126.5, 127.4, 130.2, 148.2, 149.4, 157.6. MS (EI) m/z 351 (M^+, 100%). HRMS calcd for $C_{22}H_{25}NO_3$ (M^+) 351.1834; found 351.1837.

*7,10,11-Trimethoxy-2-propyl-1,2,3,4-tetrahydrodibenzo[f,h]isoquinoline (**29b**).* Yield 13% (method n); yellow needle; mp 159−160 °C. ^{1}H NMR (400 MHz, $CDCl_3$): 1.03 (t, J = 7.6 Hz, 3H), 1.75 (sextet, J = 7.6 Hz, 2H), 2.67 (t, J = 7.6 Hz, 2H), 2.92 (t, J = 6.0 Hz, 2H), 3.24 (t, J = 6.0 Hz, 2H), 3.98 (s, 2H), 4.02 (s, 3H), 4.05 (s, 3H), 4.11 (s, 3H), 7.15 (s, 1H), 7.21 (dd, J = 9.2, 2.4 Hz, 1H), 7.89 (d, J = 2.4 Hz, 1H), 7.91 (s, 1H), 7.93 (d, J = 9.2 Hz, 1H). ^{13}C NMR (150 MHz, $CDCl_3$): 12.0, 20.4, 26.9, 50.2, 53.9, 55.5, 55.8, 55.9, 60.5, 103.7, 103.8, 104.6, 114.8, 123.3, 123.9, 124.0, 125.0, 126.0, 126.8, 130.1, 148.3, 149.3, 157.4. MS (EI) m/z 365 (M^+, 100%). HRMS calcd for $C_{23}H_{27}NO_3$ (M^+) 365.1991; found 365.1995.

*2-Butyl-7,10,11-trimethoxy-1,2,3,4-tetrahydrodibenzo[f,h]isoquinoline (**29c**).* Yield 15% (method n);yellow crystal; mp 130−131 °C. ^{1}H NMR (300 MHz, $CDCl_3$): 1.00 (t, J = 7.5 Hz, 3H), 1.45 (sextet, J = 7.5 Hz, 2H), 1.71 (quintet, J = 7.5 Hz, 2H), 2.71 (t, J = 7.5 Hz, 2H), 2.92 (t, J = 5.7 Hz, 2H), 3.23 (t, J = 5.7 Hz, 2H), 3.98 (s, 2H), 4.02 (s, 3H), 4.05 (s, 3H), 4.11 (s, 3H), 7.12 (s, 1H), 7.21 (dd, J = 9.0, 2.6 Hz, 1H), 7.88 (d, J = 2.6 Hz, 1H), 7.90 (s, 1H), 7.92 (d, J = 9.0 Hz, 1H). MS (EI) m/z 379 (M^+, 88%) and 336 (100%). HRMS calcd for $C_{24}H_{29}NO_3$ (M^+) 379.2147; found 379.2136.

*2-Ethyl-6,7,11-trimethoxy-1,2,3,4-tetrahydrodibenzo[f,h]isoquinoline (**30a**).* Yield 65% (method m); yellow crystal; mp 111−112 °C. ^{1}H NMR (300 MHz, $CDCl_3$): 1.31 (t, J = 7.2 Hz, 3H), 2.79 (q, J = 7.2 Hz, 2H), 2.95 (t, J = 5.7 Hz, 2H), 3.23 (t, J = 5.7 Hz, 2H), 3.97 (s, 3H), 4.01 (s, 2H), 4.04 (s, 3H), 4.10 (s, 3H), 7.21 (dd, J = 8.9, 2.6 Hz, 1H), 7.24 (d, J = 2.6 Hz, 1H), 7.30 (s, 1H), 7.93 (s, 1H), 8.46 (d, J = 8.9 Hz, 1H). ^{13}C NMR (150 MHz, $CDCl_3$): 12.4, 27.3, 49.7, 52.3, 53.6, 55.4, 55.8, 55.9, 103.2, 103.8, 103.9, 115.0, 123.2, 124.1, 125.0, 125.5, 128.2, 130.6, 148.5, 148.7, 157.6. MS (EI) m/z 351 (M^+, 100%). HRMS calcd for $C_{22}H_{25}NO_3$ (M^+) 351.1834; found 351.1836.

*6,7,11-Trimethoxy-2-propyl-1,2,3,4-tetrahydrodibenzo[f,h]isoquinoline (**30b**).* Yield 80% (method m); yellow crystal; mp 114−115 °C. ^{1}H NMR (300 MHz, $CDCl_3$): 1.02 (t, J = 7.5 Hz, 3H), 1.75 (sextet, J = 7.5 Hz, 2H), 2.68 (t, J = 7.5 Hz, 2H), 2.94 (t, J = 6.0 Hz, 2H), 3.22 (t, J = 6.0 Hz, 2H), 3.97 (s, 3H), 4.00 (s, 2H), 4.04 (s, 3H), 4.10 (s, 3H), 7.21 (dd, J = 8.7, 2.7 Hz, 1H), 7.24 (d, J = 2.7 Hz, 1H), 7.30 (s, 1H), 7.93 (s, 1H), 8.46 (d, J = 8.7 Hz, 1H). ^{13}C NMR (150 MHz, $CDCl_3$): 11.9, 20.0, 26.5, 49.6, 53.4, 55.5, 55.8, 55.9, 59.9, 103.1, 103.5, 103.8, 115.3, 123.2, 124.1, 124.2, 124.8, 127.8, 130.3, 148.6, 148.8, 157.7. MS (EI) m/z 365 (M^+, 90%) and 336 (100%). HRMS calcd for $C_{23}H_{27}NO_3$ (M^+) 365.1991; found 365.1987.

*6,7,10-Trimethoxy-2-propyl-1,2,3,4-tetrahydrodibenzo[f,h]isoquinoline (**31**).* Yield 60% (method m); yellow needle; mp 159−160 °C. ^{1}H NMR (400 MHz, $CDCl_3$): 1.02 (t, J = 7.6 Hz, 3H), 1.74 (sextet, J = 7.6 Hz, 2H), 2.65 (t, J = 7.6 Hz, 2H), 2.93 (t, J = 6.0 Hz, 2H), 3.19 (t, J = 5.6 Hz, 2H), 4.02 (s, 3H), 4.05 (s, 5H), 4.11 (s, 3H), 7.20 (dd, J = 8.8, 2.4 Hz, 1H), 7.30 (s, 1H), 7.81 (d, J = 8.8 Hz, 1H), 7.90 (d, J = 2.4 Hz, 1H), 7.91 (s, 1H). MS (EI) m/z 365 (M^+, 100%). HRMS calcd for $C_{23}H_{27}NO_3$ (M^+) 365.1991; found 365.1998.

*7,8,11-Trimethoxy-2-propyl-1,2,3,4-tetrahydrodibenzo[f,h]isoquinoline (**32**).* Yield 51% (method m); yellow crystal; mp 88−89 °C. ^{1}H NMR (300 MHz, $CDCl_3$): 1.01 (t, J = 7.5 Hz, 3H), 1.74 (sextet, J = 7.5 Hz, 2H), 2.66 (t, J = 7.8 Hz, 2H), 2.90 (t, J = 5.7 Hz, 2H), 3.21 (t, J = 5.7 Hz, 2H), 3.89 (s, 3H), 3.96 (s, 2H), 3.98 (s, 3H), 4.02 (s, 3H), 7.21 (d, J = 2.9 Hz, 1H), 7.24 (dd, J = 10.4, 2.9 Hz, 1H), 7.27 (d, J = 9.0 Hz, 1H), 7.75 (d, J = 9.0 Hz, 1H), 9.62 (d, J = 10.4 Hz, 1H). ^{13}C NMR (150 MHz, $CDCl_3$): 12.1, 20.5, 27.6, 50.2, 54.2, 55.3, 56.3, 59.7, 60.7, 104.2, 111.7, 113.8, 119.5, 122.8, 124.0, 125.9, 126.6, 128.8, 129.8, 132.9, 146.3, 151.0, 157.9. MS (EI) m/z 365 (M^+, 86%) and 336 (100%). HRMS calcd for $C_{23}H_{27}NO_3$ (M^+) 365.1991; found 365.1987.

*6,7,8,10,11-Pentamethoxy-2-propyl-1,2,3,4-tetrahydrodibenzo-[f,h]isoquinolin-4-ol (**33a**).* Yield 20% (method n), light-yellow crystal; mp 213−214 °C. ^{1}H NMR (600 MHz, $CDCl_3$): 1.01 (t, J = 7.8 Hz, 3H), 1.72 (sextet, J = 7.8 Hz, 2H), 2.54 (dd, J = 11.1, 2.1 Hz, 1H), 2.59 (ddt, J = 15.3, 12, 7.8 Hz, 1H), 2.68 (ddt, J = 15.3, 12, 7.8 Hz, 1H), 3.35 (d, J = 11.1 Hz, 1H), 3.47 (d, J = 15.3 Hz, 1H), 3.97 (s, 3H), 4.00 (s, 3H), 4.05 (s, 3H), 4.06 (s, 3H), 4.09 (s, 3H), 4.11 (d, J = 15.3 Hz, 1H), 5.09 (s, 1H), 6.96 (s, 1H), 7.64 (s, 1H), 9.16 (s, 1H). ^{13}C NMR (150 MHz, $CDCl_3$): 11.9, 20.0, 54.4, 55.6, 55.7, 55.8, 57.9, 60.1, 60.5, 61.3, 64.9, 101.4, 102.5, 107.8, 118.2, 123.9, 124.4, 127.7, 128.1, 128.3, 142.2, 147.9, 148.5, 151.4, 151.9. MS (EI) m/z 441 (M^+, 61%) and 370 (100%). HRMS calcd for $C_{25}H_{31}NO_6$ (M^+) 441.2151; found 441.2149.

*2-Ethyl-7,10,11-trimethoxy-1,2,3,4-tetrahydrodibenzo[f,h]isoquinolin-4-ol (**33b**).* Yield 31% (method n); yellow needle; mp 207−208 °C. ^{1}H NMR (300 MHz, $CDCl_3$): 1.28 (t, J = 7.2 Hz, 3H), 2.38 (dd, J = 11.4, 2.4 Hz, 1H), 2.60 (ddq, J = 14.7, 12.3, 7.2 Hz, 1H), 2.78 (ddq, J = 14.7, 12.3, 7.2 Hz, 1H), 3.18 (d, J = 14.7 Hz, 1H), 3.36 (d, J = 11.4 Hz, 1H), 3.62 (d, J = 14.7 Hz, 1H), 3.91 (s, 3H), 4.03 (s, 3H), 4.10 (s, 3H), 5.05 (s, 1H), 6.53 (s, 1H), 7.24 (dd, J = 9.3, 2.7 Hz, 1H), 7.64 (s, 1H), 7.72 (d, J = 2.7 Hz, 1H), 8.34 (d, J = 9.3 Hz, 1H). ^{13}C NMR (150 MHz, $CDCl_3$): 12.1, 52.1, 53.7, 55.5, 55.8, 55.9, 57.3, 64.3, 103.0, 103.6, 104.5, 115.1, 124.1, 124.5, 124.7, 126.0, 126.2, 128.2, 130.6, 148.7, 149.2, 157.6. MS (EI) m/z 367 (M^+, 42%) and 310 (100%). HRMS calcd for $C_{22}H_{25}NO_4$ (M^+) 367.1784; found 367.1780.

*7,10,11-Trimethoxy-2-propyl-1,2,3,4-tetrahydrodibenzo[f,h]isoquinolin-4-ol (**33c**).* Yield 16% (method n); yellow needle; mp 209−210 °C. ^{1}H NMR (600 MHz, $CDCl_3$): 1.01 (t, J = 7.2 Hz, 3H), 1.70−1.75 (m, 2H), 2.46 (d, J = 11.4 Hz, 1H), 2.51−2.56 (m, 1H), 2.63−2.68 (m, 1H), 3.29 (d, J = 14.4 Hz, 1H), 3.34 (d, J = 11.4 Hz, 1H), 3.81 (d, J = 14.4 Hz, 1H), 3.96 (s, 3H), 4.03 (s, 3H), 4.10 (s, 3H), 5.08 (s, 1H), 6.71 (s, 1H), 7.25 (dd, J = 9.0, 3.0 Hz, 1H), 7.72 (s, 1H), 7.78 (d, J = 1.8 Hz, 1H), 8.32 (d, J = 8.4 Hz, 1H). ^{13}C NMR (150 MHz, $CDCl_3$): 12.0, 19.7, 53.9, 55.5, 55.7, 55.8, 57.8, 60.4, 64.4, 102.9, 103.4, 104.3, 114.9, 124.0, 124.3, 124.7, 125.9, 126.3, 128.0, 130.5, 148.6, 149.0, 157.5. LRMS (EI^+) m/z (rel intensity) 381 (M^+, 42%) and 310 (100%). HRMS calcd for $C_{23}H_{27}NO_4$ (M^+) 381.1940; found, 381.1936.

*2-Butyl-7,10,11-trimethoxy-1,2,3,4-tetrahydrodibenzo[f,h]isoquinolin-4-ol (**33d**).* Yield 14% (method n); light-yellow crystal; mp 165−166 °C. ^{1}H NMR (600 MHz, $CDCl_3$): 1.01 (t, J = 7.2 Hz, 3H), 1.41−1.45 (m, 2H), 1.66−1.70 (m, 2H), 2.42 (d, J = 11.4 Hz, 1H), 2.50−2.55 (m, 1H), 2.64−2.69 (m, 1H), 3.22 (d, J = 15.6 Hz, 1H), 3.35 (d, J = 12.0 Hz, 1H), 3.67 (d, J = 14.4 Hz, 1H), 3.94 (s, 3H), 4.02 (s, 3H), 4.10 (s, 3H), 5.05 (s, 1H), 6.61 (s, 1H), 7.24 (dd, J = 9.0, 3.0 Hz, 1H), 7.68 (s, 1H), 7.75 (d, J = 1.8 Hz, 1H), 8.33 (d, J = 9.6 Hz, 1H). ^{13}C NMR (150 MHz, $CDCl_3$): 14.1, 20.8, 28.5, 53.9, 55.5, 55.7, 55.8, 57.8, 58.3, 64.3, 102.8, 103.3, 104.3, 114.9, 123.9, 124.2, 124.8, 125.9, 126.4, 127.9, 130.5, 148.5, 148.9, 157.5. LRMS (EI^+) m/z (rel intensity) 395 (M^+, 10%) and 310 (100%). HRMS calcd for $C_{24}H_{29}NO_4$ (M^+) 395.2097; found, 395.2098.

Biology. *Statistical Analysis.* InStat version 3.06 software for Windows (GraphPad, San Diego, CA) was used to evaluate the statistical significance between two groups by 2-tailed unpaired Student's t test. Throughout the text, figures, and legends, the following terminology is used to denote statistical significance: $^*p < 0.001$; $^\#p < 0.01$; ns, no significance.

Western Analysis. These assays were performed as described.[5,23,26] Cyclin A2, c-Jun, iNOS, COX-2, and GAPDH proteins were analyzed by immunoblotting with anti-Cyclin A2, anti-c-Jun (Santa Cruz Biotechnology, Santa Cruz, CA), anti-iNOS (BIOMOL Research

Laboratories, Plymouth Meeting, PA), anti-COX-2 (Upstate Biotechnology), and anti-GAPDH (Cell Signaling, Beverly, MA) antibodies, respectively.

In Vitro Carcinoma Cell Growth Inhibitory Assay. The previously described assay procedure was used.[23,27] The human lung carcinoma cell line A549 cells (ATCC CCL-185) were grown in normal RPMI 1640 culture medium (GIBCO-Life Technologies, Inc., Gaithersburg, MD) supplemented with 2 g/L of $NaHCO_3$, 2 mM L-glutamine, and 10% fetal bovine serum (FBS, Hyclone Laboratory Inc., Greeley, Co). NUGC-3 gastric carcinoma, HONE-1 nasopharyngeal carcinoma, MCF-7 breast carcinoma, NCI-H460 lung carcinoma, SF-268 glioblastoma, HepG2 hepato carcinoma, and A549 lung carcinoma cells were seeded at 4500, 6000, 6500, 2500, 7500, 10000, and 5000 cells/well, respectively, in 96-well plates. The positive control paclitaxel was purchased from Calbiochem-EMD Millipore (cat. 580555) with purity of ≥97% by HPLC.

In Vitro Anti-inflammatory Effect by Determining Nitric Oxide Production. The previously described assay procedure was employed.[5,28] RAW264.7 cells were seeded (65000 cells/well) and cultured in 96-well plates. After 24 h incubation, the medium was replaced with complete medium containing IFNγ (20 ng/mL)/LPS (5 μg/mL), and the test compounds were added at various concentrations as indicated for 18 h before measurement of nitric oxide production by the Nitrate/Nitrite assay kit as described.

Immunofluorescent Assay (IFA). The IFA assay was performed and the images were captured as described.[26] Briefly, ST cells in 96-well plates, with or without a 2 h pretreatment with test compounds, were infected with TGEV at a multiplicity of infection (MOI) of 10 for IFA. The IFA was performed at 6 h postinfection (hpi) with antibodies against the spike (S) and nucleocapsid (N) proteins of TGEV. The cells were treated with 10 different concentrations of test compounds. The results of these assays were used to obtain the dose−response curves from which 50% maximal effective concentration (EC_{50}) values were determined.

Cytopathic Effect Induced by Murine Hepatitis Virus in DBT Cells. The murine astrocytoma cell line DBT (a kind gift from Dr. Lai, Michael M. C.; Academia Sinica, Taiwan, R.O.C.)[29] and embryonic murine hepatocyte cell line BNL CL.2 (BCRC no. 60180) was maintained as monolayer culture in Dulbecco's Modified Eagles Medium (DMEM, Hyclone Laboratory Inc., Greeley, Co) supplemented with 10% heat-inactivated FBS. The murine hepatitis virus (MHV), JHM strain (a gift from Dr. Jan, Jia-Tsrong; Academia Sinica, Taiwan, R.O.C.), was propagated in BNL CL.2 cells[30] and harvested and the viral titer was measured. The DBT culture condition and the MOI of MHV-JHM used were optimized and determined in order to induce evident cytopathic effects at 24 hpi. DBT cells (2.8×10^5 cells/well) were seeded onto the 24-well plates the day before infection with MHV-JHM. Prior to the addition of test compounds, the culture medium was changed to DMEM containing 2% FBS for MHV-JHM infection. The test compounds were pretreated for 1 h prior to MHV-JHM infection at MOI of 0.005, and the cytopathic effects in DBT cells were observed at 24 hpi and recorded using a charge-coupled device linked to a Nikon Eclipse TE2000 microscopy. Subsequently, these MHV-infected DBT cells were subject to immunofluorescent assay as described above with a monoclonal antibody against MHV N protein generated in our laboratory (data not shown and will publish elsewhere).

Animal Study Protocols. Animal study protocols [(NHRI-IACUC-096006-A, 04/20/2007−04/19/2010), (NHRI-IACUC-096036-A, 11/01/2007−10/31/2010), (NHRI-IACUC-099025-A, 04/20/2010−04/19/2013), (NHRI-IACUC-099047-A, 10/31/2010−10/31/2013), (NHRI-IACUC-100112-A, 01/01/2012−12/31/2015), and (NHRI-IACUC-099065-A, 08-10-2010−08-09-2013)] were reviewed and approved for the in vivo experiments herein by the Institutional Animal Care and Use Committee of National Health Research Institutes, Taiwan.

Pharmacokinetic Analysis. The Sprague−Dawley rats for the pharmacokinetic study were obtained from BioLASCO Taiwan Co. (Ilan, Taiwan) and housed in the animal facility at the National Health Research Institutes, Taiwan. The animal studies were performed according to committee-approved procedures. Male rats (330−380 g, 9−10 weeks old) were quarantined for 1 week before use. The animals were surgically implanted with a jugular vein cannula 1 day before treatment and were fasted before treatment. Compounds **10b**, **29a**, and **33b** at 3 mg/kg as well as tylophovatine C at 1.5 mg/kg were given to rats ($n = 3$) by intravenous or oral administration as prepared in a mixture of DMA/PEG400 (30/70, v/v) for **10b**, **29a**, and **33b** and of DMA/PEG400 (50/50, v/v) for tylophovatine C. The volume of the dosing solution given was adjusted according to the body weight recorded before the drug was administered. At 0 (immediately before dosing), 2, 5 (intravenous only), 15, and 30 min and 1, 2, 4, 6, 8, 12, and 24 h after compound administration, a blood sample (150 μL) was taken from each animal via the jugular vein cannula and stored in ice (0−4 °C). The processing of the plasma and subsequent analysis by high performance liquid chromatography-tandem mass spectrometry (HPLC-MS) were as described.[31] The plasma concentration data were analyzed by a standard noncompartmental method with the Kinetica software (InnaPhase, Philadelphia, PA, USA).

In Vivo Anti-inflammatory Activity Measured by Carrageenan-Induced Hind-Paw Edema Test in Rats. Female Sprague−Dawley rats (193−214 g, 8−9 week old, $n = 5$) were used. To produce inflammation, 100 μL of 1% carrageenan solution in normal saline was injected into the left hind paw subplantar tissue. One hour before carrageenan challenge, the sample preparations (3 or 5 mg/kg) were injected intraperitoneally to the divided groups, with DMSO (100 μL) injected into the vehicle control group. The tests were performed as described.[28] The positive control indomethacin was purchased from Sigma-Aldrich (cat. I7378) with purity of ≥99% (TLC). When inhibition is or greater than 30%, the treatment is considered with a significant efficacy.

In Vivo Antitumor Activity. Four week-old male nude mice (Nu-*Foxn1*^{nu}, BioLASCO Taiwan Co., Ltd.) were used. Nude mice were subcutaneously injected with 10 million A549 cells (in 200 μL of RPMI-1640 medium) into the right flank. When the average size of tumors reached ∼60 mm^3, mice were randomly divided into three groups ($n = 8$ for treatments of vehicle and **33b** at the dose of 10 mg/kg; $n = 7$ for treatment of **33b** at the dose of 5 mg/kg) and treated with vehicle control (25% DMA + 75% PEG400), **33b** (5 mg/kg), and **33b** (10 mg/kg) via oral gavage. Each group was administered once daily, on day 1−10, day 15−19, and day 22−26, for 20 times in total. The tumor volume was calculated using the equation V (mm^3) = $a \times b^2/2$, where a is the largest diameter and b is the smallest diameter.[32] Tumor growth inhibitions (TGI) were determined for antitumor effects which are expressed as % $(T_{day60} - T_{day1})/C_{day60} - C_{day1})$ (T/C, treated versus control), dividing the tumor volumes from treatment groups with the control groups and multiplied by 100%. The effective criteria for the T/C (%) according to the National Cancer Institute standard is <42%.[33] The reduction in tumor volume for treated versus vehicle treatment should be greater than 58% to be considered with a significant efficacy. No overt signs of any adverse were observed from the test mice during experimental period.

Rota-Rod Test for Motor Coordination. Neurotoxicity was determined by a rota-rod test for motor coordination. Male nude mice were used in antitumor test first as described above and subsequently for the rota-rod test with modification.[25] The mice tested included four groups. Group I: tumor-bearing mice received vehicle (25% DMA + 75% PEG400, $n = 8$). Group II: tumor-bearing mice received **33b** at dose of 5 mg/kg for 20 administrations ($n = 7$). Group III: tumor-bearing mice received **33b** at dose of 10 mg/kg for 20 administrations ($n = 8$). Group IV: the same age of normal nude mice ($n = 5$) without tumor or any treatment as another control group in addition to group I. On the day of 58−61 after the compound or vehicle administrations, all the mice were placed onto individual sections of the apparatus for training (day 58) and test (day 59, 60, and 61) with the rod setting in motion at a increscent speed from 2 to 30 rpm in 300 s. Performance was measured as the time that elapsed between the animal being placed on the rod and falling off the rotating rod with 300 s as the cutoff.

■ ASSOCIATED CONTENT

Supporting Information

One-dimensional, two-dimensional NMR data of **33a** and experimental details for intermediates **14a−14c**, **15a−15c**, **16a−16d**, **22a−22d**, **23a−23e**, **24a−24e**, **25a−25e**, **26a−26e**, **19**, **20**, **21**, **22e**, **7a−7l**, and **27a−27k** This material is available free of charge via the Internet at http://pubs.acs.org.

■ AUTHOR INFORMATION

Corresponding Author

*Phone: 886-37-246166 ext 35715. Fax: 886-37-586456. E-mail: slee@nhri.org.tw.

Notes

The authors declare no competing financial interest.

■ ACKNOWLEDGMENTS

This work was supported by the National Health Research Institutes, Taiwan, R.O.C., and by the National Science Council of Taiwan, R.O.C. (99-320-B-400-010-MY3). Cheng-Wei Yang and Ya-Qi Qiu currently are Ph.D. students in the Graduate Program of Biotechnology in Medicine sponsored by the National Tsing Hua University and the National Health Research Institutes. The authors acknowledge Dr. Iou-Jiun Kang for support with a part of ^{1}H NMR, ^{13}C NMR, and LC/MS measurements and Dr. Yu-Chen Chou a part of the ^{1}H NMR and LC/MS measurements. We are also grateful to Dr. Jinq-Chyi Lee for proof reading the manuscript.

■ ABBREVIATIONS USED

A549, human lung adenocarcinoma epithelial cells; AP1, activator protein 1; CC_{50}, concentration of 50% cellular cytotoxicity; DBT, murine astrocytoma cells; GAPDH, glyceraldehyde 3-phosphate dehydrogenase; GI_{50}, concentration required for 50% inhibition of cell growth; HepG2, human liver hepatocellular carcinoma cells; HONE-1, human nasopharyngeal cells; LPS, lipopolysaccharides; MCF-7, human breast carcinoma cells; MHV, murine hepatitis virus; N, nucleocapsid; NCI-H460, human nonsmall cell lung cancer cells; NF-κB, nuclear factor κ-light chain-enhancer of activated B cells; NUGC-3, human gastric carcinoma cells; RAW264.7, murine macrophage; S, spike; SD, standard deviation; SF-268, human glioblastoma cells; ST, swine testicular epithelial cells; TGEV, transmissible gastroenteritis coronavirus

■ REFERENCES

(1) Huang, X.; Gao, S.; Fan, L.; Yu, S.; Liang, X. Cytotoxic Alkaloids from the Roots of *Tylophora atrofolliculata*. *Planta Med.* **2004**, *70*, 441−445.

(2) Chemler, S. R. Phenanthroindolizidines and Phenanthroquinolizidines: Promising Alkaloids for Anti-Cancer Therapy. *Curr. Bioactive Compd.* **2009**, *5*, 2−19.

(3) Lee, Y. Z.; Huang, C. W.; Yang, C. W.; Hsu, H. Y.; Kang, I. J.; Chao, Y. S.; Chen, I. S.; Chang, H. Y.; Lee, S. J. Isolation and Biological Activities of Phenanthroindolizidine and Septicine Alkaloids from the Formosan *Tylophora Ovata*. *Planta Med.* **2011**, *77*, 1932−1938.

(4) Li, Z.; Jin, Z.; Huang, R. Isolation, Total Synthesis and Biological Activity of Phenanthroindolizidine and Phenanthroquinolizidine Alkaloids. *Synthesis* **2001**, *16*, 2365−2378.

(5) Yang, C. W.; Chen, W. L.; Wu, P. L.; Tseng, H. Y.; Lee, S. J. Anti-Inflammatory Mechanisms of Phenanthroindolizidine Alkaloids. *Mol. Pharmacol.* **2006**, *69*, 749−758.

(6) Yang, C. W.; Chuang, T. H.; Wu, P. L.; Huang, W. H.; Lee, S. J. Anti-Inflammatory Effects of 7-Methoxycryptopleurine and Structure−Activity Relations of Phenanthroindolizidines and Phenanthroquinolizidines. *Biochem. Biophys. Res. Commun.* **2007**, *354*, 942−948.

(7) Gao, W.; Lam, W.; Zhong, S.; Kaczmarek, C.; Baker, D. C.; Cheng, Y. C. Novel Mode of Action of Tylophorine Analogs as Antitumor Compounds. *Cancer Res.* **2004**, *64*, 678−688.

(8) Yang, C. W.; Lee, Y. Z.; Kang, I. J.; Barnard, D. L.; Jan, J. T.; Lin, D.; Huang, C. W.; Yeh, T. K.; Chao, Y. S.; Lee, S. J. Identification of Phenanthroindolizines and Phenanthroquinolizidines as Novel Potent Anti-Coronaviral Agents for Porcine Enteropathogenic Coronavirus Transmissible Gastroenteritis Virus and Human Severe Acute Respiratory Syndrome Coronavirus. *Antiviral Res.* **2010**, *88*, 160−168.

(9) Kimball, F. S.; Turunen, B. J.; Ellis, K. C.; Himes, R. H.; Georg, G. I. Enantiospecific Synthesis and Cytotoxicity of 7-(4-Methoxyphenyl)-6-phenyl-2,3,8,8a-tetrahydroindolizin-5(1*H*)-One Enantiomers. *Bioorg. Med. Chem.* **2008**, *16*, 4367−4377.

(10) Lin, J. C.; Yang, S. C.; Hong, T. M.; Yu, S. L.; Shi, Q.; Wei, L.; Chen, H. Y.; Yang, P. C.; Lee, K. H. Phenanthrene-Based Tylophorine-1 (PBT-1) Inhibits Lung Cancer Cell Growth through the Akt and NF-κB Pathways. *J. Med. Chem.* **2009**, *52*, 1903−1911.

(11) Kimball, F. S.; Himes, R. H.; Georg, G. I. Synthesis and Evaluation of Heteroaromatic 6,7-Diaryl-2,3,8,8a-tetrahydroindolizin-5(1*H*)-Ones for Cytotoxicity against the HCT-116 Colon Cancer Cell Line. *Bioorg. Med. Chem. Lett.* **2008**, *18*, 3248−3250.

(12) Wei, L.; Brossi, A.; Kendall, R.; Bastow, K. F.; Morris-Natschke, S. L.; Shi, Q.; Lee, K. H. Antitumor Agents 251: Synthesis, Cytotoxic Evaluation, and Structure−Activity Relationship Studies of Phenanthrene-Based Tylophorine Derivatives (PBTs) as a New Class of Antitumor Agents. *Bioorg. Med. Chem.* **2006**, *14*, 6560−6569.

(13) Wei, L.; Shi, Q.; Bastow, K. F.; Brossi, A.; Morris-Natschke, S. L.; Nakagawa-Goto, K.; Wu, T. S.; Pan, S. L.; Teng, C. M.; Lee, K. H. Antitumor Agents 253. Design, Synthesis, and Antitumor Evaluation of Novel 9-Substituted Phenanthrene-Based Tylophorine Derivatives as Potential Anticancer Agents. *J. Med. Chem.* **2007**, *50*, 3674−3680.

(14) Fu, Y.; Lee, S. K.; Min, H. Y.; Lee, T.; Lee, J.; Cheng, M.; Kim, S. Synthesis and Structure−Activity Studies of Antofine Analogues as Potential Anticancer Agents. *Bioorg. Med. Chem. Lett.* **2007**, *17*, 97−100.

(15) Suffness, M.; Douros, J. *Anticancer Agents Based on Natural Product Models*; Academic Press: New York, 1980; pp 465−487.

(16) Chuang, T. H.; Lee, S. J.; Yang, C. W.; Wu, P. L. Expedient Synthesis and Structure−Activity Relationships of Phenanthroindolizidine and Phenanthroquinolizidine Alkaloids. *Org. Biomol. Chem.* **2006**, *4*, 860−867.

(17) Duclos, R. I., Jr.; Tung, J. S.; Rapoport, H. A High-Yield Modification of the Pschorr Phenanthrene Synthesis. *J. Org. Chem.* **1984**, *49*, 5243.

(18) Buckley, T. F., III; Rapoport, H. A-Amino Acids as Chiral Educts for Asymmetric Products, Chirally Specific Syntheses of Tylophorine and Cryptopleurine. *J. Org. Chem.* **1983**, *48*, 4222−4232.

(19) Su, C. R.; Damu, A. G.; Chiang, P. C.; Bastow, K. F.; Morris-Natschke, S. L.; Lee, K. H.; Wu, T. S. Total Synthesis of Phenanthroindolizidine Alkaloids (±)-Antofine, (±)-Deoxypergularinine, and Their Dehydro Congeners and Evaluation of Their Cytotoxic Activity. *Bioorg. Med. Chem.* **2008**, *16*, 6233−6241.

(20) Wang, K.; Lu, M.; Yu, A.; Zhu, X.; Wang, Q. Iron(III) Chloride Catalyzed Oxidative Coupling of Aromatic Nuclei. *J. Org. Chem.* **2009**, *74*, 935−938.

(21) Bremmer, M. L.; Khatri, N. A.; Weinreb, S. M. Quinolizidine Alkaloid Synthesis Via the Intramolecular Imino Diels−Alder Reaction. *epi*-Lupinine and Cryptopleurine. *J. Org. Chem.* **1983**, *48*, 3661−3666.

(22) Yang, X.; Shi, Q.; Bastow, K. F.; Lee, K. H. Antitumor Agents. 274. A New Synthetic Strategy for E-Ring SAR Study of Antofine and Cryptopleurine Analogues. *Org. Lett.* **2010**, *12*, 1416−1419.

(23) Wu, C. M.; Yang, C. W.; Lee, Y. Z.; Chuang, T. H.; Wu, P. L.; Chao, Y. S.; Lee, S. J. Tylophorine Arrests Carcinoma Cells at G1 Phase by Downregulating Cyclin A2 Expression. *Biochem. Biophys. Res. Commun.* **2009**, *386*, 140−145.

(24) Lee, S. J.; Wu, C. M.; Yang, C. W. Tylophorine Elevates the Amounts of c-Jun Protein in Carcinoma Cells. ASCB 47th Annual Meeting, Washington, DC, December 1−5, 2007.
(25) Jones, B. J.; Roberts, D. J. The Quantiative Measurement of Motor Inco-Ordination in Naive Mice Using an Acelerating Rotarod. *J. Pharm. Pharmacol.* **1968**, *20*, 302−304.
(26) Yang, C. W.; Yang, Y. N.; Liang, P. H.; Chen, C. M.; Chen, W. L.; Chang, H. Y.; Chao, Y. S.; Lee, S. J. Novel Small-Molecule Inhibitors of Transmissible Gastroenteritis Virus. *Antimicrob. Agents Chemother.* **2007**, *51*, 3924−3931.
(27) Chang, H. S.; Lin, Y. J.; Lee, S. J.; Yang, C. W.; Lin, W. Y.; Tsai, I. L.; Chen, I. S. Cytotoxic Alkyl Benzoquinones and Alkyl Phenols from Ardisia Virens. *Phytochemistry* **2009**, *70*, 2064−2071.
(28) Tseng, H. Y.; Wu, S. H.; Huang, W. H.; Wang, S. F.; Yang, Y. N.; Mahindroo, N.; Hsu, T.; Jiaang, W. T.; Lee, S. J. Benzothiazolium Compounds: Novel Classes of Inhibitors That Suppress the Nitric Oxide Production in RAW264.7 Cells Stimulated by LPS/IFNγ. *Bioorg. Med. Chem. Lett.* **2005**, *15*, 2027−2032.
(29) Koetters, P. J.; Hassanieh, L.; Stohlman, S. A.; Gallagher, T.; Lai, M. M. Mouse Hepatitis Virus Strain JHM Infects a Human Hepatocellular Carcinoma Cell Line. *Virology* **1999**, *264*, 398−409.
(30) O'Keefe, B. R.; Giomarelli, B.; Barnard, D. L.; Shenoy, S. R.; Chan, P. K.; McMahon, J. B.; Palmer, K. E.; Barnett, B. W.; Meyerholz, D. K.; Wohlford-Lenane, C. L.; McCray, P. B., Jr. Broad-Spectrum in Vitro Activity and in Vivo Efficacy of the Antiviral Protein Griffithsin against Emerging Viruses of the Family Coronaviridae. *J. Virol.* **2010**, *84*, 2511−2521.
(31) Yao, H. T.; Wu, Y. S.; Chang, Y. W.; Hsieh, H. P.; Chen, W. C.; Lan, S. J.; Chen, C. T.; Chao, Y. S.; Chang, L.; Sun, H. Y.; Yeh, T. K. Biotransformation of 6-Methoxy-3-(3′,4′,5′-trimethoxy-benzoyl)-1*H*-Indole (BPR0L075), a Novel Antimicrotubule Agent, by Mouse, Rat, Dog, and Human Liver Microsomes. *Drug Metab. Dispos.* **2007**, *35*, 1042−1049.
(32) Yang, R.; Rescorla, F. J.; Reilly, C. R.; Faught, P. R.; Sanghvi, N. T.; Lumeng, L.; Franklin, T. D., Jr.; Grosfeld, J. L. A Reproducible Rat Liver Cancer Model for Experimental Therapy: Introducing a Technique of Intrahepatic Tumor Implantation. *J. Surg. Res.* **1992**, *52*, 193−198.
(33) Bissery, M. C.; Chabot, G. G. History and New Development of Screening and Evaluation Methods of Anticancer Drugs Used in Vivo and in Vitro. *Bull. Cancer* **1991**, *78*, 587−602.